TTMP vol 1(2), 2024
doi: 10.30511/TTMP.2024.2016004.1019

Transactions in Theoretical and Mathematical Physics

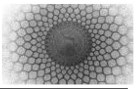

Solutions of generalized supergravity equations with the BTZ black hole metric

A. Eghbali[a], **S. Ghasemi-Sorkhabi**[b], **A. Rezaei-Aghdam**[c]

Department of Physics, Azarbaijan Shahid Madani University, 53714-161, Tabriz, Iran

Received: 19 November 2023 / Accepted: 03 February 2024 / Published: 25 February 2024

Abstract

We proceed to investigate the solutions of generalized supergravity equations (GSE) in three dimensions. Our candidate is the metric of BTZ black hole. It is shown that only the cases with $J = M = 0$ and $J = 0,\ M \neq 0$ of the BTZ metric satisfy the GSE. In the former, we find a family of solutions including the field strength $H_{r\varphi t} = 2r/l$, the cosmological constant $\Lambda = -1/l^2$, one-form Z_μ and a vector field which is obtained to be a linear combination of the directions of the time translation and rotational symmetries. In the latter, the solutions possess the same field strength as before, while the cosmological constant Λ, one-form Z_μ and vector field I will be different from the previous case. Finally, we show that the charged black string solution found by Horne and Horowitz, which is Abelian T-dual to the the BTZ black hole solution, can be considered as a solution for the GSE.

Keywords: Generalized supergravity equations; Standard supergravity; BTZ metric

1 Introduction

Supergravity is a modern field theory combining the principles of supersymmetry and general relativity. The 10- dimensional supergravity theory describes the dynamics of massless string excitations and arises in string theory as a low-energy effective theory. Recently, new string backgrounds have been discovered that satisfy a more general set of motion equations than ordinary supergravity. These equations, which are a generalization of the standard supergravity equations, are called the GSE. It's worth noting that the primary difference between standard supergravity and GSE is the absence of a scalar dilaton. Arutyunov, *et al.* [1] introduced the GSE in order to investigate integrable deformations of the $AdS_5 \times S^5$ type II superstring sigma model [2, 3][1], which is closely related to non-Abelian T-duality transformations [10–13]. This generalized system in string theory includes additional vector fields I in addition to the standard component fields of type IIB supergravity. Up to now, the corresponding classical action has not been discovered, and only the equations of motion are presented. Additionally, Ref. [14] presents a solution of standard supergravity with a linear dilaton that has been mapped to a GSE solution through a formal T-duality transformation along a specific direction. These findings emphasize the importance of treating solutions of standard supergravity and GSE equally in the context of string theory, as T-duality is a fundamental symmetry in string theory. As a great progress in the recent study of string theory, Tseytlin and Wulff [15] demonstrated that the GSE can be reproduced by solving the κ-symmetry constraints. In fact, their results show that the κ-symmetry of the Green-Schwarz action requires the background supergravity fields to satisfy the GSE.

Later, the GSE attracted the attention of many researchers, in such a way that it was shown that [16] the whole bosonic part of the type II GSE can be reproduced from the T-duality covariant equations of motion of the double field theory when one chooses a non-standard solution of the strong constraint. Additionally, in Ref. [16], the Weyl invariance of the bosonic sigma model on a generalized gravity background has been

[a]Corresponding author: eghbali978@gmail.com
[b]s.ghassemi.s@gmail.com
[c]rezaei-a@azaruniv.ac.ir

[1]In order to construct the Yang-Baxter deformations of $AdS_5 \times S^5$, one must employ the classical r-matrix as a solution of the homogeneous classical Yang-Baxter equation [4]. It has been shown that the Yang-Baxter deformed background of $AdS_5 \times S^5$ satisfies the equations of motion of type IIB supergravity if the classical r-matrix satisfies the unimodularity condition [5] (see, also, [6–9]). Otherwise, the background is a solution of the GSE.

shown by using the doubled formalism. We think that the results of work of Ref. [16] have provided positive evidence that superstring theories defined on solutions of the GSE are Weyl invariant (see, also, [17]). In Ref. [18], without introducing a T-duality manifest formulation of string theory, it has been constructed a local counterterm that cancels out the Weyl anomaly of bosonic string theory defined in generalized supergravity backgrounds; the results of their work support the Weyl invariance of string theory in generalized supergravity backgrounds. Also, it has been shown that the equations of motion of generalized supergravity can be followed from the sigma model once the Killing vector I is identified with the trace of the structure constants [12]. In this regard, for the Bianchi spacetimes, it was shown that [12] the non-Abelian T-duals with respect to non-semisimple groups are solutions to generalized supergravity.

As a spin off from this progress, it would be interesting to present new solutions for the GSE in three dimensions. In this work, we obtain some new solutions for the GSE, including special cases of the BTZ metric ($J = M = 0$ and $J = 0,\ M \neq 0$). Notably, when we select the vector field I based on our perspective, it becomes evident that the cases with $J \neq 0, M = 0$ and $J \neq 0,\ M \neq 0$ do not satisfy the GSE. As an interesting result, we show that the charged black string solution found by Horne and Horowitz [19], which is Abelian T-dual to the the BTZ black hole solution, can be considered as a solution for the GSE.

The structure of the paper is as follows. We start with a short overview of the GSE in section 2, and introduce our notation. Next, in section 3, after the introduction of the BTZ black hole metric, we consider the BTZ black hole solutions in the context of the low energy approximation. Section 4 contains the original results of the work: we look into the BTZ metrics in the context of the GSE and show that only the cases $J = M = 0$ and $J = 0,\ M \neq 0$ of the BTZ metric can satisfy the GSE. In section 5, the charged black string solution is considered as a solution for the GSE. Finally, conclusion is reported in section 6.

2 A brief review of the GSE

The subject of this section is a brief overview of the GSE. In the absence of Ramond-Ramond fields, these equations in D dimensions take the following form [1]

$$R_{\mu\nu} - \tfrac{1}{4}\, H_{\mu\rho\sigma}\, H_{\nu}^{\rho\sigma} + (\nabla_\mu\, X_\nu + \nabla_\nu\, X_\mu) = 0, \tag{1}$$

$$\tfrac{1}{2}\nabla^\lambda\, H_{\lambda\mu\nu} - X^\lambda\, H_{\lambda\mu\nu} - \nabla_\mu\, X_\nu + \nabla_\nu\, X_\mu = 0, \tag{2}$$

$$R - \tfrac{1}{12}H^2 + 4\nabla_\mu\, X^\mu - 4X_\mu\, X^\mu - 4\,\Lambda = 0, \tag{3}$$

where $R_{\mu\nu}$ and R are the respective Ricci tensor and Gauss curvature that are calculated from the metric $G_{\mu\nu}$, and Λ is the cosmological constant. Here, the D-dimensional indices $\mu,\ \nu, \ldots$ of coordinates x^μ are raised or lowered with the metric $G_{\mu\nu}$. The covariant derivative ∇_μ is the conventional Levi-Civita connection associated with $G_{\mu\nu}$. The field strength $H_{\mu\nu\rho}$ corresponding to anti-symmetry tensor field B is defined as

$$H_{\mu\nu\rho} = \partial_\mu\, B_{\nu\rho} + \partial_\nu\, B_{\rho\mu} + \partial_\rho\, B_{\mu\nu}. \tag{4}$$

In addition, X_μ is defined to be $X_\mu = I_\mu + Z_\mu$ in which $I = I^\mu\ \partial_\mu$ is a vector field, while $Z = Z_\mu\ dx^\mu$ is a one-form. They satisfy [1]

$$\mathscr{L}_I\ \ G_{\mu\nu} = 0, \tag{5}$$

$$\mathscr{L}_I\ \ B_{\mu\nu} = 0, \tag{6}$$

$$\nabla_\mu\ \ Z_\nu - \nabla_\nu\, Z_\mu + I^\lambda\, H_{\lambda\mu\nu} = 0, \tag{7}$$

$$I^\lambda\ \ Z_\lambda = 0, \tag{8}$$

where $\mathscr{L}$ stands for the Lie derivative. The conventional dilaton is included in Z_μ as follows:

$$Z_\mu = \partial_\mu\, \Phi + B_{\nu\mu}\, I^\nu. \tag{9}$$

Here, Φ is a scalar dilaton field hidden within Z_μ. Note that if we set $I^\mu = 0$, then one gets that $X_\mu = \partial_\mu\, \Phi$, and thus, the GSE reduce to the standard supergravity equations.

In this work, we present new solutions for the GSE (1)-(3) together with (5)-(8), including special cases of the BTZ metric, field strength H, one-form Z_μ, and an appropriate vector field I. In this manner, we will derive a family of solutions for the cases $J = 0,\ M = 0$ and $J = 0,\ M \neq 0$ within the BTZ metric. As mentioned earlier, the case $I^\mu = 0$ of the GSE corresponds to the standard supergravity equations. It has already been shown that [20] a slight modification of the BTZ black hole solution yields an exact solution to the standard supergravity equations. In the next section, after a brief overview of the BTZ black hole, we consider the BTZ metric in the context of the low energy approximation.

3 The BTZ black hole metric as a solution of the standard supergravity equations

First of all, let us introduce the metric of BTZ black hole. The BTZ black hole, discovered by Banados, Teitelboim, and Zanelli [21], is a $2+1$-dimensional solution of Einstein's equations with negative cosmological constant, mass, angular momentum, and charge. Unlike its higher-dimensional counterparts, the BTZ black hole is asymptotically anti-de Sitter and lacks a curvature singularity at the origin. The line element for the black hole solutions is as follows [21]:

$$ds^2 = (M - \frac{r^2}{l^2})\, dt^2 - J\, dt\, d\varphi + r^2\, d\varphi^2 + (\frac{r^2}{l^2} - M + \frac{J^2}{4r^2})^{-1}\, dr^2, \qquad 0 \le \varphi \le 2\pi. \tag{10}$$

where the radius l is related to the cosmological constant by $l = (-\Lambda)^{-1/2}$. The constants of motion, denoted by M and J, represent the mass and angular momentum of the BTZ black hole, respectively. The line element (10) describes a black hole solution with outer and inner horizons at $r = r_+$ and $r = r_-$, respectively,

$$r_\pm = l\Big(\frac{M}{2}\Big)^{1/2}\Big\{1 \pm \Big(1 - \frac{J^2}{M^2 l^2}\Big)^{1/2}\Big\}^{1/2}. \tag{11}$$

The mass M and angular momentum J are related to $r = r_\pm$ by $M = (r_+^2 + r_-^2)/l^2$ and $J = 2\, r_+\, r_-/l^2$. Solutions with $-1 < M < 0$ and $J = 0$ describe point particle sources with naked conical singularities at $r = 0$. The metric with $J = 0$ and $M = -1$ can be recognized as ordinary anti-de Sitter space, and it is separated by a mass gap from the case where $J = 0$ and $M = 0$. The vacuum state, representing empty space, is obtained by letting the horizon size go to zero. This corresponds to $M \to 0$, which requires $J \to 0$. It's worth noting that the metric for the $J = 0$ and $M = 0$ black hole is not the same as the AdS_3 metric, which has negative mass, $M = -1$.

As mentioned in the previous section, a modified BTZ black hole solution was obtained to a $2+1$-dimensional string theory with a matter source given by anti-symmetric B-field with the contribution of the cosmological constant Λ [20]. There, Horowitz and Welch showed that very solution to 3-dimensional general relativity with $\Lambda < 0$ can be considered as a solution to the standard supergravity equations with a constant dilaton field, $\Lambda = -1/l^2$ and field strength $H_{\mu\nu\rho} = 2\varepsilon_{\mu\nu\rho}/l$, where $\varepsilon_{\mu\nu\rho}$ stands for the volume form in three dimensions[2]. In addition, it was shown that [20] the solution of BTZ black hole (10) along with a constant dilaton field, $\Lambda = -1/l^2$ and field strength $H_{r\varphi t} = 2r/l$ satisfy the equations of motion of the standard supergravity. It is worth mentioning that 3-dimensional black hole solutions to (10) do not exist assumed that $H_{\mu\nu\rho} = 0$.

4 Solutions of the GSE with the BTZ metric

In what follows we shall look into the BTZ solutions in the context of the GSE. We show that the cases $J = M = 0$ and $J = 0,\ M \neq 0$ of the BTZ metric can be considered as solutions of the GSE. As mentioned in section 3, the M and J are the mass and angular momentum of the BTZ black hole, respectively. They are appeared due to the time translation symmetry and rotational symmetry of the metric, corresponding to the Killing vectors $\partial/\partial t$ and $\partial/\partial\varphi$, respectively. On the other hand, relation (5) is called Killing equation, which in terms of a Killing vector field $K_a = K_a{}^\mu \partial_\mu$ it can be written as

$$\partial_\mu K_a{}^\lambda\, G_{\lambda\nu} + K_a{}^\lambda \partial_\lambda G_{\mu\nu} + \partial_\nu K_a{}^\lambda\, G_{\mu\lambda} = 0. \tag{12}$$

Accordingly, the vector field I can be a Killing vector or a linear combination of the Killing vectors corresponding to metric (10). The Killing vectors K_a corresponding to the BTZ metric can be derived by solving Killing equation (12), giving us six linearly independent vectors. Here, to construct an appropriate vector field I we use the Killing vectors of the BTZ metric. We assume that the choice of

$$I = \alpha_1 K_1 + \cdots + \alpha_6 K_6, \tag{13}$$

for some constants α_i, can be a suitable candidate for solving the GSE (1)-(3) together with (5)-(8). It should be noted the fact that the BTZ solutions must be single-valued in the angular direction. Therefore, one should be careful in choosing the vector field I. As the first example, we look into the case $J = 0, M = -\lambda^2 < 0$ of (10) in full detail.

4.1 Solutions with J=0, M=-$\lambda^2 < 0$

In this subsection we shall investigate the solutions of the GSE for the case $J = 0, M = -\lambda^2 < 0$ of the BTZ metric. Before proceeding to do this, let us first write down the BTZ metric for the case $J = 0, M = -\lambda^2 < 0$. Using relation (10), it is given by

$$ds^2 = -(\lambda^2 + \frac{r^2}{l^2})\, dt^2 + (\lambda^2 + \frac{r^2}{l^2})^{-1}\, dr^2 + r^2\, d\varphi^2. \tag{14}$$

The Killing vectors of the metric (14) can be derived by solving Killing equations. They are then read off

$$K_1 = \frac{\partial}{\partial\varphi},$$

$$K_2 = \sqrt{\lambda^2 l^2 + r^2}\ \Big[\frac{rl}{\lambda^2 l^2 + r^2}\ \cos(\frac{\lambda t}{l})\sin(\lambda\varphi)\ \frac{\partial}{\partial t} + \lambda \sin(\frac{\lambda t}{l})\sin(\lambda\varphi)\frac{\partial}{\partial r} + \frac{1}{r}\sin(\frac{\lambda t}{l})\cos(\lambda\varphi)\frac{\partial}{\partial\varphi}\Big],$$

$$K_3 = \sqrt{\lambda^2 l^2 + r^2}\ \Big[-\frac{rl}{\lambda^2 l^2 + r^2}\ \sin(\frac{\lambda t}{l})\sin(\lambda\varphi)\ \frac{\partial}{\partial t} + \lambda \cos(\frac{\lambda t}{l})\sin(\lambda\varphi)\frac{\partial}{\partial r} + \frac{1}{r}\cos(\frac{\lambda t}{l})\cos(\lambda\varphi)\frac{\partial}{\partial\varphi}\Big],$$

$$K_4 = \sqrt{\lambda^2 l^2 + r^2}\ \Big[-\frac{rl}{\lambda^2 l^2 + r^2}\ \cos(\frac{\lambda t}{l})\cos(\lambda\varphi)\ \frac{\partial}{\partial t}$$

[2]Note that a special property of three dimensions is that the field strength $H_{\mu\nu\rho}$ must be proportional to the volume form $\varepsilon_{\mu\nu\rho}$.

$$-\lambda \sin(\frac{\lambda t}{l})\cos(\lambda\varphi)\frac{\partial}{\partial r}+\frac{1}{r}\sin(\frac{\lambda t}{l})\sin(\lambda\varphi)\frac{\partial}{\partial\varphi}\Big],$$

$$K_5=\sqrt{\lambda^2 l^2+r^2}\ \Big[\frac{rl}{\lambda^2 l^2+r^2}\ \sin(\frac{\lambda t}{l})\cos(\lambda\varphi)\ \frac{\partial}{\partial t}$$
$$-\lambda\cos(\frac{\lambda t}{l})\cos(\lambda\varphi)\frac{\partial}{\partial r}+\frac{1}{r}\cos(\frac{\lambda t}{l})\sin(\lambda\varphi)\frac{\partial}{\partial\varphi}\Big],$$

$$K_6=-l^2\frac{\partial}{\partial t}. \tag{15}$$

Fortunately, for integer values of λ, the resulting Killing vectors are single-valued in the angular direction. Now, we apply the Killing vectors (15) to construct an appropriate vector field by using formula (13). As we will see, our solutions are classified into two special cases. In both cases of solutions, the anti-symmetry tensor field B is considered to be $B=-r^2/l\ dt\wedge d\varphi$. Then, one can employ formula (5) to calculate the field strength corresponding to this B-field, giving us

$$H=-\frac{2r}{l}\ dr\wedge dt\wedge d\varphi. \tag{16}$$

Here, the forms of our solutions including the metric (14) and field strength (16) are given by the following two cases I and II:

• Case I: In this case, the GSE (1)-(3) together with (5)-(8) are fulfilled with the metric (14) and field strength (16) if the vector field I, one-form Z and cosmological constant Λ can now be expressed in the following forms

$$I=-\alpha_6 l^2\ \frac{\partial}{\partial t},\quad Z=\alpha_6 l r^2\ d\varphi,\quad \Lambda=-\frac{1}{l^2}+\lambda^2{\alpha_6}^2 l^4. \tag{17}$$

Using these, the dilaton field is constant, and the components of X_μ read off

$$X_t=\alpha_6 l^2(\lambda^2+\frac{r^2}{l^2}),\quad X_\varphi=\alpha_6 l r^2,\quad X_r=0. \tag{18}$$

• Case II: In this case of solutions, the vector field I is a rotational symmetry, which together with one-form Z and Λ are given as follows:

$$I=\alpha_1\ \frac{\partial}{\partial\varphi},\quad Z=\alpha_1 l(\lambda^2+\frac{r^2}{l^2})dt,\quad \Lambda=-\frac{1}{l^2}+\lambda^2{\alpha_1}^2 l^2. \tag{19}$$

Then, one finds that

$$X_t=\alpha_1 l(\lambda^2+\frac{r^2}{l^2}),\quad X_\varphi=\alpha_1 r^2,\quad X_r=0. \tag{20}$$

The corresponding dilaton field to this case of the solutions is time-dependent, $\Phi=c_0+\lambda^2\alpha_1 lt$.

Let us now discuss the solutions for all positive and negative values of M, when J is zero. The BTZ metric with $J=0, M\neq 0$ is given by

$$ds^2=(M-\frac{r^2}{l^2})\ dt^2+(\frac{r^2}{l^2}-M)^{-1}\ dr^2+r^2\ d\varphi^2. \tag{21}$$

In this case, the solutions are similar to those of the case $J=0, M=-\lambda^2$, so that one should use M instead of $-\lambda^2$ in the solutions (17) and (19). Then, the solutions take the forms

$$I=-\alpha_6 l^2\ \frac{\partial}{\partial t},\quad Z=\alpha_6 l r^2\ d\varphi,\quad \Lambda=-\frac{1}{l^2}-M{\alpha_6}^2 l^4, \tag{22}$$

and

$$I=\alpha_1\ \frac{\partial}{\partial\varphi},\quad Z=\alpha_1 l(\frac{r^2}{l^2}-M)dt,\quad \Lambda=-\frac{1}{l^2}-M{\alpha_1}^2 l^2, \tag{23}$$

and in the same way for the components of X_μ.

4.2 Solution with J=0, M=0

The BTZ metric with $J=0,\ M=0$ is simply found by using the formula (10), giving us

$$ds^2=-\frac{r^2}{l^2}\ dt^2+\frac{l^2}{r^2}\ dr^2+r^2\ d\phi^2. \tag{24}$$

In order to construct the vector field I, one may determine the Killing vectors corresponding to the metric (24) similar to what was done in (15). Analogously, only non-zero component of the tensor field B is considered to be $B_{\varphi t}=r^2/l$ for which the field strength is calculated to be as in (16). Now, we solve the GSE with the metric (24), field strength (16) and a constant dilaton field. The equations are then satisfied if the vector field I, one-form Z and Λ have the following forms[3]

$$I=-\alpha_6 l^2\ \frac{\partial}{\partial t}+\alpha_3\ \frac{\partial}{\partial\varphi},$$

$$Z=\frac{\alpha_3 r^2}{l}dt+\alpha_6 l r^2 d\varphi,$$

$$\Lambda=-\frac{1}{l^2}. \tag{25}$$

Using the first two relations and also the B-field $B_{\varphi t}=r^2/l$, one then finds that the components of X_μ are

$$X_t=(\alpha_3+\alpha_6 l)\ \frac{r^2}{l},$$

$$X_\varphi=(\alpha_3+\alpha_6 l)\ r^2,$$

$$X_r=0. \tag{26}$$

[3]Note that our solution including the metric (24), $B_{\varphi t}=r^2/l$ and relations given by equation (25) together with a constant dilaton field may be related to a GSE solution found in equation (4.12) of Ref. [22]. There, it has been obtained a 10-dimensional solution for the GSE (with a non-zero Killing vector I) whose metric is locally $AdS_3\times S^3\times T^4$. If we look at the AdS_3 part of solution (4.12) of [22], it may be locally the same as our BTZ solution.

At the end of this section let us compare the solutions with J=0, M=0 and J=0, M≠0. As showed in the above, for the case of J=0, M=0 we obtained the vector I as a linear combination of the directions of the time translation and rotational symmetries, while this is not true for the case of J=0, M≠0. In the case M≠0 of the solutions, if one uses a linear combination of (22) and (23) for the vector I and one-form Z, then, equation (8) becomes $\alpha_1\alpha_6 l^3 M = 0$. This means that one of the constants α_1 or α_6 should be zero. Therefore, unlike the case of J=0, M=0, a linear combination of (22) and (23) cannot be a solution for the GSE.

5 Abelian target space dual of the BTZ as a solution of the GSE

One of the interesting issues in the context of GSE is that to investigate the solutions of the GSE under the T-duality. The T-duality symmetry is one of the most interesting properties of string theory connecting seemingly different backgrounds in which the strings propagate. We say that the duality is Abelian if it is constructed on an Abelian isometry group [23]. By making use of the Buscher's duality transformations [23], it was shown that the BTZ black hole solution discussed at the end of section 3 is, under the Abelian T-duality, equivalent to the charged black string solution discussed in Ref. [19]. There, Horne and Horowitz found a family of solutions to low energy string theory describing charged black strings in three dimensions. This family of solutions is given by

$$d\tilde{s}^2 = -\big(1-\frac{\mathbf{M}}{\hat{r}}\big)d\hat{t}^2+\Big(1-\frac{\mathbf{Q}^2}{M\hat{r}}\Big)d\hat{x}^2 +\big(1-\frac{\mathbf{M}}{\hat{r}}\big)^{-1}\Big(1-\frac{\mathbf{Q}^2}{\mathbf{M}\hat{r}}\Big)^{-1}\frac{l^2 d\hat{r}^2}{4\hat{r}^2}, \tag{27}$$

$$\tilde{H} = \frac{\mathbf{Q}}{\hat{r^2}}\, d\hat{r}\wedge d\hat{t}\wedge d\hat{x}, \tag{28}$$

$$\tilde{\Phi} = -\frac{1}{2}\ln(l\hat{r}), \tag{29}$$

where $\mathbf{M} = r_+^2/l$ and $\mathbf{Q} = J/2$ are the respective the mass and charge of the black string. It can be easily shown that the above metric admits two Killing vectors $\partial/\partial\hat{t}$ and $\partial/\partial\hat{x}$. Here, we shall show that the metric (27) and field strength (28) can satisfy the GSE, if the vector field I, one-form Z, dilaton field and cosmological constant express as follows:

$$I = \alpha_1\,\frac{\partial}{\partial\hat{t}},$$

$$Z = -\frac{1}{2\hat{r}}d\hat{r}+\alpha_1\big(\frac{\mathbf{M}}{\mathbf{Q}}-\frac{\mathbf{Q}}{\hat{r}}\big)d\hat{x},$$

$$\Phi = c_0-\frac{1}{2}\ln\hat{r}+\alpha_1\frac{\mathbf{M}}{\mathbf{Q}}\hat{x},$$

$$\Lambda = \frac{2}{l^2}+\frac{2{\alpha_1}^2(\mathbf{M}^2-\mathbf{Q}^2)}{\mathbf{Q}^2}. \tag{30}$$

In addition to this solution, one can see that the GSE (1)-(3) together with (5)-(8) are fulfilled with the metric (27) and field strength (28) if the vector field I, one-form Z, dilaton field and cosmological constant can now be expressed in the following forms

$$I = \alpha_2\,\frac{\partial}{\partial\hat{x}},$$

$$Z = -\frac{1}{2\hat{r}}d\hat{r}+\alpha_2\mathbf{Q}\big(\frac{1}{\hat{r}}-\frac{1}{\mathbf{M}}\big)d\hat{t},$$

$$\Phi = c_0-\frac{1}{2}\ln\hat{r}-\alpha_2\frac{\mathbf{Q}}{\mathbf{M}}\hat{t},$$

$$\Lambda = \frac{2}{l^2}+\frac{2{\alpha_2}^2(\mathbf{M}^2-\mathbf{Q}^2)}{\mathbf{M}^2}. \tag{31}$$

6 Conclusion

In this study, we have obtained some new solutions for the GSE in three dimensions. Our solutions include the special cases $J=0, M=0$ and $J=0, M\neq 0$ of the BTZ metric together with the field strength $H=-(2r/l)dr\wedge dt\wedge d\varphi$. In each case we have calculated the the vector field I, one-form Z and the cosmological constant Λ. To determine the vector field I we have used the Killing vectors corresponding to the BTZ metrics. By comparing the solutions with $J=0, M=0$ and $J=0, M\neq 0$, we concluded that unlike the case of $J=0, M=0$, a linear combination of (22) and (23) cannot be a solution for the GSE. However, we have derived a family of solutions as presented in relations (22), (23) and (25). Notably, our results confirm that these solutions are single-valued in the angular direction. On the other hand, we have checked that the cases $J\neq 0, M=0$ and $J\neq 0, M\neq 0$ for the BTZ metric do not satisfy the GSE.

While we considered the BTZ metrics, one can easily repeat for other geometric metrics such as Thurston geometries. As mentioned in section 3, the BTZ metric with $J=0$ and $M=-1$ represents ordinary anti-de Sitter space (AdS_3), which is nothing but one of Lorentzian Thurston geometries. Therefore, we have investigated that the AdS_3 space can be considered as a solution for the GSE. Finally, as an interesting result, we have shown that the charged black string solution (27), which is Abelian T-dual to the the BTZ black hole solution, can be also a solution for the GSE. In fact, this result helps to answer the question whether the solutions of the GSE are, under the Abelian T-duality, preserved. It will be an interesting future direction to be addressed.

Acknowledgements This work has been supported by the research vice chanceller of Azarbaijan Shahid Madani University under research fund No. 1402/231.

References

1. G. Arutyunov, S. Frolov, B. Hoare, R. Roiban, A. A. Tseytlin, Nucl. Phys. B **903**, 262 (2016)
2. F. Delduc, M. Magro, B. Vicedo, Phys. Rev. Lett. **112**, 051601 (2014)
3. F. Delduc, M. Magro, B. Vicedo, J. High Energy Phys. **10**, 132 (2014)
4. I. Kawaguchi, T. Matsumoto, K. Yoshida, J. High Energy Phys. **04**, 153 (2014)
5. R. Borsato, L. Wulff, J. High Energy Phys. **10**, 045 (2016)
6. T. Araujo, I. Bakhmatov, E. O Colgain, J. Sakamoto, M. M. Sheikh-Jabbari, K. Yoshida, Phys. Rev. D **95**, 105006 (2017)
7. T. Araujo, I. Bakhmatov, E. O Colgain, J. Sakamoto, M. M. Sheikh-Jabbari, K. Yoshida, J. Phys. A **51**, 235401 (2018)
8. T. Araujo, E. O Colgain, J. Sakamoto, M. M. Sheikh-Jabbari, K. Yoshida, Eur. Phys. J. C **77**, 739 (2017)
9. I. Bakhmatov, O. Kelekci, E. O Colgain, M. M. Sheikh-Jabbari, Phys. Rev. D **98**, 021901 (2018)
10. D. Orlando, S. Reffert, J. I. Sakamoto, K. Yoshida, J. Phys. A **49**, 445403 (2016)
11. B. Hoare, A. A. Tseytlin, J. Phys. A **49**, 494001 (2016)
12. M. Hong, Y. Kim, E. O. Colgain, Eur. Phys. J. C **78**, 1025 (2018)
13. R. Borsato, L. Wulff, J. High Energy Phys. **08**, 027 (2018)
14. B. Hoare, A. A. Tseytlin, J. High Energy Phys. **10**, 060 (2015)
15. L. Wulff, A. A. Tseytlin, J. High Energy Phys. **06**, 174 (2016)
16. J. Sakamoto, Y. Sakatani, K. Yoshida, PTEP **053B07** (2017)
17. Y. Sakatani, S. Uehara, K. Yoshida, J. High Energy Phys. **04**, 123 (2017)
18. J. J. Fernandez-Melgarejo, J. Sakamoto, Y. Sakatani, K. Yoshida, Phys. Rev. Lett. **122**, 111602 (2019)
19. J. Horne and G. Horowitz, Nucl. Phys. B **368**, 444 (1992)
20. G. Horowitz, D. Welch, Phys. Rev. Lett. **71**, 328 (1993)
21. M. Banados, C. Teitelboim, J. Zanelli, Phys. Rev. Lett. **69**, 1849 (1992)
22. Y. Sakatani, Prog. Theor. Exp. Phys. **073**B04 (2019)
23. T. Buscher, Phys. Lett. B **194**, 59 (1987); Phys. Lett. B **201**, 466 (1988).

TTMP vol 1(2), 2024
doi: 10.30511/TTMP.2024.2006716.1011

Transactions in Theoretical and Mathematical Physics

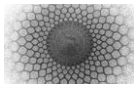

A new approach to momentum operators in curved space

M. Jafari Matehkolaee[1,a], Z. Norouzbeh[2]

[1] Department of Physics and Energy Engineering, Amir Kabir University of Technology (Tehran Polytechnic) Hafez Avenue, Tehran, Iran

[2] Physics Department, Faculty of Physics and Chemistry, Alzahra University, Vanak, 1993891176, Tehran, Iran

Received: 11 July 2023 / Accepted: 29 November 2023 / Published: 10 February 2024

Abstract In this paper, we obtained momentum representation in curved space using a distinct procedure from previous reports. Then, as a straight application for these operators, we have investigated them on the compact manifold as a sphere. Our investigation indicates that the spectrum of generalized momentum operators on the compact manifold is discrete.

1 Introduction

The "relativity revolution" and the "quantum revolution" are among the greatest successes of twentieth-century physics, yet the theories they produced appear to be fundamentally incompatible. General relativity remains a purely classical theory and describes the geometry of space and time as smooth and continuous, whereas quantum mechanics divides everything into discrete pieces. Many attempts have been made to unify two theories, and one of the ideas for unifying these theories is quantized gravity [1-4]. But in some references instead of trying to quantize the gravity, the effects of the metric have been proposed [5].

For a comprehensive understanding of the quantum mechanics in curved space, it is essential to establish a representation of the generalized momentum operators [6]. These operators must satisfy the Heisenberg commutation:

$$\left[X_i, P_j\right] = i\hbar\delta_j^i, \tag{1}$$

$$\left[P_i, P_j\right] = 0. \tag{2}$$

In a renowned paper [7], considering the aforementioned equations and concept of the delta function in curved space, the Hermitian form of the generalized momentum operator is obtained

$$P_i = -i\hbar\left(\frac{\partial}{\partial x^i} + \frac{1}{2}\Gamma_{ji}^{j}\right) = -i\hbar\frac{1}{\sqrt[4]{g}}\frac{\partial}{\partial x^i}\sqrt[4]{g}, \tag{3}$$

where $\Gamma_{ji}^{j}(x) = \frac{\partial}{\partial x^i} ln(\sqrt{g(x)})$ and g is the metric of the curved space under consideration.

In ref. [8] and [9] the non-Hermitian form of momentum operator in curved space is presented. In an approach near the report [7], equation (3) is derived without employing the delta function in curved space. However, in reference [10], a distinct approach is taken. By utilizing the matrix representation of the momentum generalized coordinates transformation, the non-Hermitian form of equation (3) is obtained. The covariant and contravariant components of the familiar form of the momentum operator $-i\hbar\vec{\nabla}$ have been formulated for curvilinear coordinates in three-dimensional space directly [11]. Recently, the representation of the inverse momentum operator in curved space has been reported [12].

This paper is organized as follows: first, in section II, we obtain equation (3) with a different procedure, which is mentioned in the various references. In Section III, as an application of this relation, we examine a quantum particle on a sphere.

2 Momentum operator in curved space

A To any vector $|u\rangle$ in the Hilbert space, corresponds a function u such that

$$u(x) = \langle x|u\rangle. \tag{4}$$

The operators K_j, A_j and B_j operate on the vectors of the Hilbert space, while D_j represents the standard partial differentiation that operates on functions. Obviously, it is desired that K_j's are anti-Hermitian and satisfy

$$[X^j, K_l] = -\delta_l^j. \tag{5}$$

Defining A_j 's through

[a] m.matehkolaee@aut.ac.ir

$$\langle x|A_j|u\rangle = \big(D_j u\big)(x), \tag{6}$$

we have

$$\langle x|X^j A_l|u\rangle = x^j\langle x|A_l|u\rangle = x^j(D_l u)(x). \tag{7}$$

Also, one can write

$$\langle x|A_l X^j|u\rangle = (D_l u^j)(x), \tag{8}$$

where $\left|u^j\right\rangle = X^j|u\rangle$ and $u^j(x) = x^j u(x)$. It follows:

$$(D_l u^j)(x) = \delta_l^j u(x) + x^j(D_l u)(x). \tag{9}$$

We can also write

$$\langle x|[X^j, A_l]|u\rangle = -\delta_l^j u(x) = -\delta_l^j\langle x|u\rangle, \tag{10}$$

which shows that

$$[X^j, A_l] = -\delta_l^j. \tag{11}$$

The lastest equation resembles to equation (5) where A is replaced by K, although A is not necessarily Hermitian. By defining B through $B_j = K_j - A_j$ it becomes evident that

$$[X^j, B_l] = 0. \tag{12}$$

Therefore, B_j's are functions of X, namely $B_j = F_j(X)$. The remaining task is to determine B_j's so that K_j's becomes anti-Hermitian.

If the inner product is

$$\langle u|v\rangle = \int d^n x g^{\frac{1}{2}}(x)\overline{u(x)}v(x), \tag{13}$$

where g is the metric of the curved space under consideration. Assuming $g^{\frac{1}{2}}$ being real and positive, we can write

$$\begin{aligned}\langle u|K_j|v\rangle &= \int d^n x g^{\frac{1}{2}}(x)\overline{u(x)}[(D_j v)(x) + F_j(x)v(x)]\\ &= \int d^n x g^{\frac{1}{2}}(x)\Big\{-\overline{D_j u(x)}\\ &- (g^{\frac{-1}{2}}D_j g^{\frac{1}{2}})(x)\overline{u(x)} + F_j(x)\overline{u(x)}\Big\}v(x).\end{aligned} \tag{14}$$

Anti – Hermiticity of K_j means

$$\langle u|K_j|v\rangle = -\overline{\langle v|K_j|u\rangle}. \tag{15}$$

So, using

$$\begin{aligned}&\overline{\langle v|K_j|u\rangle} =\\ &\int d^n x g^{\frac{1}{2}}(x)\overline{u(x)}\overline{[(D_j u)(x) + \overline{F_j(x)u(x)}]v(x)}\,,\end{aligned} \tag{16}$$

one can see that

$$F_j + \overline{F_j} = g^{\frac{-1}{2}}D_j g^{\frac{1}{2}}. \tag{17}$$

That is

$$Re(F_j) = g^{\frac{-1}{4}}D_j g^{\frac{1}{4}}. \tag{18}$$

The determination of the imaginary part of F_j isn't dictated by this method. A straightforward option is to set it to zero. In this case K_j 's do commute with each other. The final result is

$$\langle x|K_j|u\rangle = g^{\frac{-1}{4}}(x)\left[D_j\left(g^{\frac{1}{4}}u\right)\right](x). \tag{19}$$

The equation (19) is completely consistent with Eq. (3).

3 Application of Momentum operator in curved space

Applying equation (3) we consider a particle constrained to the surface of a sphere an established example for quantum mechanics in curved space. The motion of constrained particle on two-dimensional sphere have been investigated in [13]. The coherent states for a particle on a sphere can be seen that in [14]. In general, there has also been a discussion about the behavior of the operator (3) on boundary conditions [15].

The adequate generalized coordinates to describe the dynamics on a sphere are $\varphi \in [0,2\pi]$, the polar angle $\theta \in [0,\pi]$ in spherical coordinates and also the radial coordinate r remains restricted to fixed radius $r = R$. The classical Hamiltonian function for a particle of mass M moving freely on this surface is then given by

$$H = \frac{1}{2MR^2}\left(p_\theta^2 + \frac{p_\varphi^2}{sin^2\,\theta}\right), \tag{20}$$

where $p_\varphi = \hat{k}.\vec{L}$ and $p_\theta = -\hat{\varphi}.\vec{L}$ describe the components of the angular momentum $\vec{L}$ with respect to the unit vectors $\hat{k}$ and $\hat{\varphi}$.

The consistent quantum mechanical Hamiltonian to the equation (20) is as follows [16,17]

$$H = \frac{1}{2MR^2}\left(g^{ij}(\theta,\varphi)p_i p_j\right). \tag{21}$$

Comparing the equation (21) with the equation (20), we can identify the metric components

$$g^{\theta\theta}(\theta,\varphi) = 1, \tag{22}$$

$$g^{\varphi\varphi}(\theta,\varphi) = \frac{1}{sin^2\,\theta}, \tag{23}$$

$$g^{\theta\varphi}(\theta,\varphi) = g^{\varphi\theta}(\theta,\varphi) = 0. \tag{24}$$

From above equations we can infer the covariant components $g_{\theta\theta}(\theta,\varphi) = 1$, $g_{\varphi\varphi}(\theta,\varphi) = sin^2\,\theta$ and $g_{\theta\varphi}(\theta,\varphi) = g_{\varphi\theta}(\theta,\varphi) = 0$ which yield the metric determinant

$$g(\theta,\varphi) = \begin{vmatrix} 1 & 0 \\ 0 & sin^2\,\theta \end{vmatrix} = sin^2\,\theta\,. \tag{25}$$

The identity operator expressed in terms of the coordinate basis reads as [7,8]

$$1 = \int dx\sqrt{g(x)}\,|x\rangle\langle x|. \tag{26}$$

Therefore to the equation (26), the identity operator in the coordinate basis $|\theta,\varphi\rangle$ is given by

$$1 = \int_0^\pi d\theta \int_0^{2\pi} d\varphi\, sin\,\theta\,|\theta,\varphi\rangle\,\langle\theta,\varphi|. \tag{27}$$

In addition to this, from the equation (3), conjugate momentum operators are

$$p_\varphi = \frac{\hbar}{i}\frac{\partial}{\partial\varphi}, \quad p_\theta = \frac{\hbar}{i}\left(\frac{\partial}{\partial\theta} + \frac{1}{2}cot\,\theta\right). \tag{28}$$

As we can obtain the eigenfunctions of the equation (3) [7], the eigenfunctions of (28) are given by

$$\langle\theta,\varphi|m_\theta,m_\varphi\rangle = \frac{e^{2im_\theta\theta}}{\sqrt{\pi\,sin\,\theta}}\frac{e^{im_\varphi\varphi}}{\sqrt{2\pi}}, \tag{29}$$

where m_θ, m_φ are the corresponding to related eigenvalues and $m_\theta, m_\varphi \in \mathbb{Z}$, so we have

$$p_\theta|m_\theta,m_\varphi\rangle = 2\hbar m_\theta|m_\theta,m_\varphi\rangle, \tag{30}$$

$$p_\varphi|m_\theta,m_\varphi\rangle = \hbar m_\varphi|m_\theta,m_\varphi\rangle \tag{31}$$

The eigenvectors form a discrete orthonormal basis of the Hilbert space

$$1 = \sum_{m_\theta\in\mathbb{Z}}\sum_{m_\varphi\in\mathbb{Z}}|m_\theta,m_\varphi\rangle\,\langle m_\theta,m_\varphi|, \tag{32}$$

$$\langle m_\theta,m_\varphi|m'_\theta,m'_\varphi\rangle = \delta_{m_\theta,m'_\theta}\delta_{m_\varphi,m'_\varphi}, \quad . \tag{33}$$

Unlike in the unbounded configuration space, the discrete momentum spectrum implies a discrete momentum subspace coordinate. This characteristic is a generic feature of compact coordinates and also arises, e.g., in the case of a single angle variable (motion on a circle) [18] or the orientation state of a rigid body. We emphasize that this discreetness does not arise due to the subspace formalism; rather, it emerges as a necessary physical consequence, as reflected in the discrete measurement outcomes of the corresponding momentum observables.

4 Conclusion

We were able to obtain equation (3) using a completely different approach from what has been done so far. Subsequently, as a straight application of operator (3), we examined their eigenstates on the sphere. It is interesting that these eigenstates are discrete while this does not happen on unbounded spaces.

References

1. L. Viola, R. Onofrio, Phys. Rev. D **55**, (1996)
2. J. F. Doonoghue and B. R. Holstein, Am. J. Phys. **54**, 9 (1986)
3. Y. Q. Cai, G. Papini, Gen. rel. and Grav. **22**, 3 (1990)
4. A. Karamatskou, H. Klinert, Int. J. Geom. Methods. Phys. **11**, 8 (2014)
5. C. C. Barros Jr, Eur. Phys. J. C **42** (2005)
6. W. Pauli, *General Principles of Quantum Mechanics*, (Springer – Verlag, New York, 1980)
7. B. S. DeWitt, T. Stanev, Phys. Rev. **85**, 653 (1952)
8. M. Carreau, Phys. Rev. D **40**, 6 (1989)

9. C. S. Wang, Am. J. Phys. **57**, 1 (1989)
10. P. V. Gonzalez, J. C. Parra, Am. J. Phys. **49**, 8 (1981)
11. B. Leaf, Am. J. Phys. **47**, 9 (1979)
12. M. Jafari Matehkolaee, Pramana J. Phys. **93**, 84 (2019)
13. L Jahangiri, H. Panahi, Ann. Phys. **375** (2016)
14. K. Kowalski, J. Rembielinski, J. Phys. A. **33** (2000)
15. M. Jafari Matehkolaee, Pramana J. Phys. **95**, 131(2021)
16. G. R. Gruber, Found. of Phys. **6**, 1 (1976).
17. J. M. Domingos, M. H. Caldeira, Found. of Phys. **14**, 7 (1984)
18. I. Rigas, L. L. Sanchez-Soto, A. B. Klimov, J. Rhehacek, Z. Hradil, Ann. Phys. **326**, 426 (2011)

TTMP vol 1(2), 2024
doi: 10.30511/TTMP.2024.2016571.1020

Transactions in Theoretical and Mathematical Physics

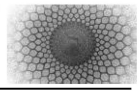

Modified geometrical optics in a curved spacetime

Mohammad Mehdi Baghaiefard[a]

Department of Physics, Isfahan University of Technology, Isfahan, Iran

Received: 12 December 2023 / Accepted: 10 March 2024 / Published: 12 March 2024

Abstract In this article, the propagation of high-frequency monochromatic beam of circularly polarized electromagnetic waves in a curved spacetime has been studied. At first, the standard geometrical optics is investigated; That is, we consider the waves with infinitely high frequency. In this step, it is found that the trajectories of light are null geodesics. Secondly, the geometrical optics is modified. For this end, by considering the polarization of light, helicity-dependent correction on the geometrical optics is included. As a result, we realize that the modified wave vector is null. Furthermore, the trajectories of light are null non-geodesic paths.
Keywords: *Circular Polarization, Helicity, Curved Spacetime, Geometrical Optics, Modified Geometrical Optics.*

1 Introduction

The propagation of circularly polarized beam of light in a gravitational field has been a matter of study in the past several years [1–6]. As we know, the propagation of electromagnetic waves in general relativity is obtained by investigating Maxwell equations in a curved spacetime. But, finding an exact solution to Maxwell equations in such spaces is a formidable problem. When the electromagnetic wave is highly monochromatic over a region of spacetime, we use an asymptotic short-wave approximation. In quantum mechanics, this method is known as WKB approximation and in wave optics is called geometrical optics approximation. This approximation is valid when the reduced wavelength (wavelength/2π) is much smaller than any characteristic scales (such as the curvature of the wave front, the size and duration of the radiation beam and the radius of the spacetime curvature) in the problem. we begin with the Maxwell equations in a curved spacetime. we write the Lorenz condition and wave equation for the potential 1-form. we select an ansatz for the potential and put it in the Lorenz condition and wave equation. Investigating these equations, we conclude that in the leading order of the geometrical optics approximation, light ray paths are null geodesics [7]. But, if the light frequency is very high but it is finite, we modify the geometrical optics by including helicity-dependent corrections on phase function of the potential ansatz. What we have done here is somehow different from what has been presented in [5] in that we directly modify the wave vector, and we find that this modified vector, corrected up to the first order of expansion parameter, is null; Also, we find that the ray trajectories of circularly polarized light in this approach are null but not geodesic.

In this article, the metric has signature $(-,+,+,+)$, vectors and differential forms are denoted by boldface letters, the inner product of two vectors $\boldsymbol{a}$ and $\boldsymbol{b}$ is defined as $(\boldsymbol{a},\boldsymbol{b}) = g_{\mu\nu}a^{\mu}b^{\nu}$, with $\boldsymbol{a}^2 = (\boldsymbol{a},\boldsymbol{a})$ and we shall use geometrized units $c = G = 1$.

2 Null Tetrads and Maxwell Equations

2.1 Null tetrads and Polarization forms

Here, we use the Newman-Penrose formalism, a tetrad formalism with a special choice of the basis vectors $\{\boldsymbol{l},\boldsymbol{n},\boldsymbol{m},\bar{\boldsymbol{m}}\}$, of which $\boldsymbol{l}$,$\boldsymbol{n}$ are real and $\boldsymbol{m}$,$\bar{\boldsymbol{m}}$ are complex conjugates of one another. They are required to satisfy the orthogonality conditions,

$$(\boldsymbol{l},\boldsymbol{m}) = (\boldsymbol{l},\bar{\boldsymbol{m}}) = (\boldsymbol{n},\boldsymbol{m}) = (\boldsymbol{n},\bar{\boldsymbol{m}}) = 0, \tag{1}$$

besides the conditions,

$$(\boldsymbol{l},\boldsymbol{l}) = (\boldsymbol{n},\boldsymbol{n}) = (\boldsymbol{m},\boldsymbol{m}) = (\bar{\boldsymbol{m}},\bar{\boldsymbol{m}}) = 0, \tag{2}$$

[a]mehdi.baghaiefard@ph.iut.ac.ir

that the vectors be null. We impose further normalization conditions as

$$(\boldsymbol{l},\boldsymbol{n})=-1,\quad (\boldsymbol{m},\bar{\boldsymbol{m}})=1. \tag{3}$$

It is necessary to mention that there are some freedoms in selecting such null tetrads. For example, to construct the vector $\boldsymbol{m}$, we have the freedom $\boldsymbol{m}\to e^{i\psi(\boldsymbol{x})}\boldsymbol{m}$, where ψ is an arbitrary function. But, the validity of our framework to measure the changes of quantities is guaranteed when the size and angle between the basis vectors do not change along the trajectory of light; Also, they are required to be rotation free, which means if the basis vector is initially tangent to the ray, it will remain tangent during the motion. But, the operator that can satisfy our needs from a basis vector is the Fermi-Walker derivative. Fermi-Walker transportation of the bases imposes some conditions which fix gauge ambiguity in the choice of these bases. Volume 4-form and three polarization 2-forms $\boldsymbol{\pi}^{(a)}$, $a=0,1,2$, are defined as [5]:

$$\boldsymbol{e}=i\boldsymbol{l}\wedge\boldsymbol{m}\wedge\bar{\boldsymbol{m}}\wedge\boldsymbol{n}, \tag{4}$$

$$\boldsymbol{\pi}^{(0)}=\bar{\boldsymbol{m}}\wedge\boldsymbol{n},\ \ \boldsymbol{\pi}^{(1)}=-(\boldsymbol{l}\wedge\boldsymbol{n}-\boldsymbol{m}\wedge\bar{\boldsymbol{m}}),\ \ \boldsymbol{\pi}^{(2)}=\boldsymbol{l}\wedge\boldsymbol{m}. \tag{5}$$

For the electromagnetic field 2-form $\boldsymbol{F}$, Maxwell equations in the absence of electric currents can be written as $d\boldsymbol{F}=\delta\boldsymbol{F}=0$, in which d is differential operator, $\delta:=\star d\star$ is codifferential operator and $\star$ is the Hodge star operator. We define [5]:

$$\boldsymbol{\mathscr{F}}^{\sigma}=\frac{1}{2}\left[\boldsymbol{F}-i\sigma(\star\boldsymbol{F})\right], \tag{6}$$

in which $\sigma=+1$ is the helicity parameter of the field related to right-handed and $\sigma=-1$ is related to left-handed circularly polarized waves. Since in our 4-dimensional spacetime with the defined signature we have $\star\star\boldsymbol{F}=-\boldsymbol{F}$, we can write $\star\boldsymbol{\mathscr{F}}^{\sigma}=i\sigma\boldsymbol{\mathscr{F}}^{\sigma}$. Then, $\boldsymbol{\mathscr{F}}^{+1}$ and $\boldsymbol{\mathscr{F}}^{-1}$ are self-dual and anti-self-dual complex electromagnetic fields, respectively. For these fields we have $d\boldsymbol{\mathscr{F}}^{\sigma}=\delta\boldsymbol{\mathscr{F}}^{\sigma}=0$. Using the coefficients Φ_a^{σ}, we can express $\boldsymbol{\mathscr{F}}^{\sigma}$ in terms of the basis 2-forms $\boldsymbol{\pi}^{(a)}$ as [5]:

$$\boldsymbol{\mathscr{F}}^{\sigma}=\sum_{a=0}^{2}\Phi_a^{\sigma}\boldsymbol{\pi}^{\sigma(a)}. \tag{7}$$

Since $\boldsymbol{\mathscr{F}}^{\sigma}$ is a closed form, assuming the region we are working on is simply connected, by the use of Poincare lemma we can define the complex potential 1-form $\boldsymbol{\mathscr{A}}^{\sigma}$ as $\boldsymbol{\mathscr{F}}^{\sigma}=d\boldsymbol{\mathscr{A}}^{\sigma}$. The Lorenz gauge condition is $\delta\boldsymbol{\mathscr{A}}^{\sigma}=0$.

2.2 Field equations

We start with the following ansatz for the potential 1-form of the electromagnetic field:

$$\boldsymbol{\mathscr{A}}^{\sigma}=\boldsymbol{a}^{\sigma}e^{\frac{iS^{\sigma}}{\varepsilon}}, \tag{8}$$

in which $\boldsymbol{a}^{\sigma}$ is the complex amplitude 1-form, S is the real phase function (eikonal function) and $\varepsilon\ll 1$ is a dummy expansion parameter that helps to track order of terms: a term with ε^n, for some integer n, varies as $(\lambda\!\!\!^{-}/l_{min})^n$, where $\lambda\!\!\!^{-}/l_{min}\ll 1$. Here $\lambda\!\!\!^{-}$ is the reduced wavelength (wavelength/2π) and l_{min} is the minimal of the characteristic scales of the problem. It is important to mention that we skip the helicity index σ and our calculation will be for the wave with right-handed polarization. For left-handed one, it is necessary to change $\varepsilon\to-\varepsilon$ and $\boldsymbol{a}\to\bar{\boldsymbol{a}}$. Putting the ansatz (8) into Lorenz gauge condition gives:

$$\star(\boldsymbol{P}\wedge\star\boldsymbol{a})-i\varepsilon\star d\star\boldsymbol{a}=0, \tag{9}$$

in which $\boldsymbol{P}:=dS$ is the wave 1-form. Also, the field strength $\boldsymbol{\mathscr{F}}$ can be written as:

$$\boldsymbol{\mathscr{F}}=\frac{i}{\varepsilon}\boldsymbol{\mathscr{Z}}e^{\frac{iS}{\varepsilon}}, \tag{10}$$

in which

$$\boldsymbol{\mathscr{Z}}:=\boldsymbol{\mathscr{B}}-i\varepsilon\boldsymbol{\mathscr{C}},\quad \boldsymbol{\mathscr{B}}:=\boldsymbol{P}\wedge\boldsymbol{a},\quad \boldsymbol{\mathscr{C}}:=d\boldsymbol{a}. \tag{11}$$

It is easy to show that:

$$\delta\boldsymbol{\mathscr{F}}=-\frac{1}{\varepsilon^2}e^{\frac{iS}{\varepsilon}}\boldsymbol{j}, \tag{12}$$

in which

$$\boldsymbol{j}\overset{1}{=}-\star\left[\boldsymbol{P}\wedge\star(\boldsymbol{a}\wedge\boldsymbol{P})\right]-i\varepsilon\left[\star(\boldsymbol{P}\wedge\star d\boldsymbol{a})-\star d\star(\boldsymbol{a}\wedge\boldsymbol{P})\right], \tag{13}$$

is the truncated current 1-form up to the first order ε. Note that the symbols $\overset{0}{=}$ and $\overset{1}{=}$ indicate that we have kept the equations up to zero order and first order of the parameter ε, respectively. Maxwell equations in current free spaces are satisfied if $\boldsymbol{j}=0$. This point reaches us to the following field equation:

$$\boldsymbol{P}^2\boldsymbol{a}-i\varepsilon\Big(\left(\nabla^{\nu}P_{\nu}\right)\boldsymbol{a}+2P^{\nu}\left(\nabla_{\nu}a_{\mu}\right)\boldsymbol{e}^{\mu}\Big)\overset{1}{=}0, \tag{14}$$

in which ∇_{ν} is the covariant derivative associated with the spacetime metric $g_{\mu\nu}$ and $\boldsymbol{e}^{\mu}$ are co-frame 1-forms. It is necessary to mention that some conditions are needed to be imposed on the fields depending on the point that either they are self-dual or anti-self-dual. For the self-dual field we should have:

$$\boldsymbol{\mathscr{F}}^{+\mathbf{1}}\circ\bar{\boldsymbol{\pi}}^{(a)}=0, \tag{15}$$

in which "$\circ$" indicates the inner product of two differential 2-forms [8]. It is necessary to note that the gauge condition $\mathscr{A} \to \mathscr{A} + d\Psi$ which $\Psi := \varepsilon\psi e^{\frac{iS}{\epsilon}}$ and ψ is a scalar function, preserves the physics of the problem. This gauge condition will help us to find vector polarization in geometrical optics approximation.

3 Geometrical Optics

At first, we keep the equation (14) up to zero order of the parameter of expansion. so, we have:

$$\boldsymbol{P}^2 \overset{0}{=} 0. \tag{16}$$

This means that $\boldsymbol{P}$ is null. If we interpret $P_\alpha = \nabla_\alpha S$ as the momenta canonically conjugated to x^α, we can identified the equation (16) with the Hamilton-Jacobi equation with an effective Hamiltonian defined as follows [9]:

$$H(x^\mu, P_\mu) := \frac{1}{2} g^{\mu\nu} P_\mu P_\nu. \tag{17}$$

Let $x^\alpha(\lambda)$, which λ is an affine parameter, be an integral curve of P^α, $P^\mu = dx^\mu/d\lambda$, then the Hamiltonian equations give the trajectories of light in the geometrical optics limit:

$$\frac{D^2x^\lambda}{d\lambda^2} := \ddot{x}^\lambda + \Gamma^\lambda_{\kappa\nu}\dot{x}^\kappa\dot{x}^\nu = 0, \tag{18}$$

in which $\Gamma^\lambda_{\kappa\nu}$ are Christoffel symbols. So, in the geometrical optics approximation, the trajectories of light are null geodesics.

4 Modified Geometrical Optics

In the next step, we modify the geometrical optics by including first order correction in the wave vector. Here, different from what has been done in [5], we directly correct the wave vector as $\boldsymbol{P} = \boldsymbol{P}_0 + \varepsilon\boldsymbol{P}_1$. If we put this in the equation (14), we have:

$$\begin{aligned}&(\boldsymbol{P}_0 + \epsilon\boldsymbol{P}_1)^2 a_{0\mu} + \varepsilon(\boldsymbol{P}_0 + \epsilon\boldsymbol{P}_1)^2 a_{1\mu} \\ &- 2i\varepsilon\left[(\boldsymbol{P}_0 + \epsilon\boldsymbol{P}_1)^\nu \nabla_\nu a_{0\mu} + \frac{1}{2} a_{0\mu}\nabla^\nu(\boldsymbol{P}_0 + \epsilon\boldsymbol{P}_1)_\nu\right] \overset{1}{=} 0.\end{aligned} \tag{19}$$

Now, we split this equation order by order in ε. At first, we have $\boldsymbol{P}_0^2 = 0$. Here, we put $\boldsymbol{P}_0 = \boldsymbol{l}$. If we put this result into (19) and use the relation $a_{0\mu} = f_0 z_{0\mu}$, by some simplifications we obtain:

$$(\boldsymbol{l}, \boldsymbol{P}_1) - i\boldsymbol{l}^\nu \bar{z_0}^\mu \nabla_\nu z_{0\mu} = 0, \tag{20}$$

Using the condition (15) and the mentioned gauge condition, we can imply that $\boldsymbol{z}_0 = \boldsymbol{m}$. Therefore, we get:

$$(\boldsymbol{l}, \boldsymbol{P}_1) - i\boldsymbol{l}^\nu \bar{m}^\mu \nabla_\nu m_\mu = 0. \tag{21}$$

Using the property of Fermi-Walker transportation, the second term on the left hand side is zero, then we have $(\boldsymbol{l}, \boldsymbol{P}_1) = 0$. Therefore, we can write:

$$\boldsymbol{P}^2 \overset{1}{=} \boldsymbol{l}^2 + 2\varepsilon(\boldsymbol{l}, \boldsymbol{P}_1) = 0. \tag{22}$$

This indicate that in the modified geometrical optics, the wave vector correction up to the first order of ε is null. Up to now, we find that $\boldsymbol{P} = \boldsymbol{l} + \varepsilon\boldsymbol{P}_1$, so we have $(\boldsymbol{P} - \varepsilon\boldsymbol{P}_1)^2 = 0$. Like the geometrical optics section, we introduce the effective Hamilton-Jacobi equations, we obtain:

$$H(x^\mu, P_\mu, \varepsilon) := \frac{1}{2}(\boldsymbol{P} - \varepsilon\boldsymbol{P}_1)^2. \tag{23}$$

Inspecting the Hamilton equations, we obtain:

$$\frac{D^2x^\mu}{d\lambda^2} = \varepsilon\sigma\left(\nabla^\mu P_{1\nu} - \nabla_\nu P_1^\mu\right)\dot{x}^\nu, \tag{24}$$

Which means in modified geometrical optics the trajectories of light rays are null non-geodesics.

5 Conclusion

In this paper, the propagation of circularly polarized high-frequency electromagnetic waves in a curved spacetime was studied. It is found that in the geometrical optics limit, the trajectories of light rays are null geodesics. But, modifying the wave vector up to first order correction, a process different from what has been presented in [5], we can conclude that the modified wave vector is null and the ray trajectories of light are null non-geodesics.

References

1. V. P. Frolov and A. A. Shoom, Phys. Rev. D 84, 044026 (2011).
2. V. P. Frolov and A. A. Shoom, Phys. Rev. D 86, 024010 (2012).
3. M. A. Oancea, J. Joudioux, I. Dodin, D. Ruiz, C. F. Paganini, and L. Andersson, (2020).
4. S. R. Dolan, (2018), arXiv:1801.02273 [gr-qc].
5. V. P. Frolov, Phys. Rev. D 102, 084013 (2020).
6. M.M.Baghaiefard, *The effect of polarization on the ray trajectories of light in a curved spacetime.* M.Sc. Thesis. Department of Physics, Isfahan University of Technology, Iran (2023).
7. C. W. Misner, K, Thorne, and J, Wheeler, Gravitation (1947).
8. Benn, I.M. and Tucker, R.W. *An Introduction to Spinors and Geometry with Applications in Physics.* Adam Hilger (IOP publishing Ltd), 1987.
9. I. Arnold, *Mathematical methods of classical mechanics* (Springer, 1989).

TTMP vol 1(2), 2024
doi: 10.30511/TTMP.2024.2023459.1022

Transactions in Theoretical and Mathematical Physics

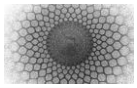

The Importance of the Domain of Operators in Quantum Mechanics

Maedeh Dolati[a], **Niloofar Parviz**

Department of Physical Chemistry and Nano Chemistry, Faculty of Chemistry, Alzahra University, Tehran, Iran

Received: 10 February 2024 / Accepted: 27 April 2023 / Published: 01 May 2024

Abstract This paper aims to examine the significance of the domain of operators in the mathematical and physical structure of quantum mechanics. Specifically, we explore the distinction between observable self-adjoint and Hermitian operators, determined by their respective domains. We also discuss the Algebra of unbounded operators with the concept of the domain of operators. Our analysis reveals that creation and annihilation operators are not generally self-adjoint towards each other in standard quantum mechanics, as demonstrated through mathematical equations.

1 Introduction

Quantum mechanics is based on the algebra of the linear operators, which are responsible for observables in the quantum world [1]. The distinction between Hermitian and self-adjoint operators is contingent upon the domain of operators, which has a vital contribution in this context. Additionally, integrable functions exhibit quadratic behaviour and do not vanish at infinity. Notably, despite this characteristic, the momentum operator does not conform to Hermiticity criteria. However, it is essential to recognize that these functions are separate from the domain of the momentum operator (as their differentiations are often non-square-integrable). Mathematicians consider every operator in Hilbert space to have two essential properties. The first is the action of an operator, and the second is its domain. The action of an operator refers to its effect on the functions it is applied to, such as differentiation or integration. An operator's domain is a specific set of functions that the operator acts on. While quantum mechanics literature often neglects to mention the domain of operators, the importance of an operator domain is highlighted in distinguishing between self-adjoint and Hermitian operators [2]. We start the discussion with the definition of the adjoint operator, which can be seen in quantum mechanics literature. However, recently, it has been reported that this subject is adjoint to an operator beyond the textbooks [3].

Definition: Assume that a densely defined operator A with domain $D(A)$, and its adjoint A^* with domain $D(A^*)$. According to the definition, the following relationship holds for all functions f and g:

$$(A * f, g) = (f, Ag). \tag{1}$$

We use a symbol like that employed in math literature for reasons that will become clear later.

Now, the following two definitions can be mentioned:
1. An (densely defined) operator A is Hermitian (or symmetric in mathematics literature) provided that its action is the same as the action of A* and $D(A) \subseteq D(A*)$. The condition $D(A) \subseteq D(A*)$follows from the definition of A^*.
2. An (densely defined) operator A is self-adjoint, again, provided that its action is the same as that of A*. But, in this case

$$D(A) = D(A*),$$

According to this definition, all bounded operators are self-adjoint.

Note that the domain of A is obtained from Eq. (1).

2 Position operator

The position operator in quantum mechanics is an unbounded operator, which is never defined on the entire Hilbert Space and inevitably, the domain related to such must be considered. This operator on the real axis is defined as follows [4]:

$$X\Psi(x) = x\Psi(x),\ x \in \mathbb{R}, \Psi(x) \in L^2(\mathbb{R}, dx), \tag{2}$$

and the domain of the position operator is equal to:

$$D(X) = \{\Psi(x) \in L^2(\mathbb{R}, dx) | \int x^2 |\Psi(x)|^2 \mathrm{dx} < \infty\}. \tag{3}$$

[a] maedehdolati.ac.ir@gmail.com

The following lemma can be deduced from the action type and the position operator's definition.

Lemma 1 *If the measurement on the position of a particle leads to an upper limit, which means:* $\lim_{x\to\infty}|x\Psi(x)| = 0$. *So, the desired continuous state function must be square integrable.*

Proof We separate the integration domain into following three parts: $[-1,1]$, $(-\infty,-1]$, $[1,+\infty)$.

For the first interval, since $\Psi(x)$ is continuous, then $|\Psi(x)|^2$ is also continuous. Therefore, $\int_{-1}^{1}|\Psi(x)|^2\,dx$ is finite. Now we examine the interval $[1,+\infty)$. From the postulation of the lemma, we conclude that there is a positive constant such as k, which can be written for all $x \geq 1$, as $|x\Psi(x)|\langle k$, so we have:

$$\int_1^{\infty}|\Psi(x)|^2 dx < \int_1^{\infty}\frac{k^2}{x^2}dx = k^2.$$

A similar argument holds for the interval $(-\infty,-1]$.

3 Momentum operator

The momentum operator is an unbounded operator whose domain is as follows [4].

$$D(P) = \{\Psi(x) \in L^2(\mathbb{R},dx)|\Psi'(x) \in L^2(\mathbb{R},dx)\}. \qquad (4)$$

It is noteworthy, concerning the domain of momentum operator, there are square-integrable functions that its derivatives do not exist in $L^2(\mathbb{R},dx)$. Hence, they do not belong in the domain of the momentum operator. For example, consider a function $f(x) = \frac{x^{\frac{1}{3}}}{1+x^2}$, despite this fact that it is considered to be a square-integrable function, but its derivative is not. Therefore, this function does not satisfy the requirement for inclusion in the domain of the momentum operator. In general, for $f(x)$ and $g(x)$ which belong to the domain of momentum operator one can write:

$$(g,Pf) - (Pg,f) = (-i\overline{g}f)_{-\infty}^{+\infty},$$

where f and g functions are often considered to be equal to zero when $x \to \pm\infty$.

It is important to note that not all square-integrable functions lead to zero, as they tend to infinity [5].

For instance, consider the function $f(x) = \sqrt{\cos x^2}$ which is square-integrable, but does not vanish when the amount of x tends to infinity. However, this is not of concern to us. In this case, see the following lemma:

Lemma 2 *Every square-integrable function that belongs to the domain of momentum operator will certainly vanish as they tend towards infinity (given their continuity and smoothness).*

Proof Consider g to be the conjugated form of function f, which is also square-integrable. Since $f \in D(P)$, then $f' \in L^2(\mathbb{R})$, and the inner product of (g,f') is well defined, we can also write:

$$(g,f') = \frac{1}{2}\int_{-\infty}^{+\infty}(f^2)'dx = f^2(+\infty) - f^2(-\infty).$$

It is clear that the limit of f^2 exists as it tends to infinity. It follows that both f^2 and $|f|^2$ tend to finite limits as infinity is approached. If any of the mentioned limits were equal to a number other than zero, the integral of $|f|^2$ would tend to infinity over the domain of real numbers, which contradicts the square-integrability of the f function. Consequently, both $|f|^2$ and $f$tend to zero when $x \to \pm\infty$.

A similar discussion but for generalized momentum operators can be found in [6].

4 Algebra of unbounded operators

The main distinction between bounded and unbounded operators lies in their domains [4]. The domain of an unbounded operator is a suitable subspace of Hilbert Space, thereby rendering certain algebraic operations such as addition and multiplication distinct from those about bounded operators. To illustrate the latter, consider two unbounded operators, A and B, and assume their sum to be $a = A + B$. According to Eq. (1) and for $f,g \in D(a)$ one can write:

$$(g,af) = (g,(A+B)f) = ((A+B)^*g,f). \qquad (5)$$

By rewriting the Eq. (5), we conclude that:

$$\big((A^*+B^*)g,f\big) = ((A+B)^*g,f). \qquad (6)$$

In this equation that A and B are unbounded, it is possible that $(A^*+B^*)g$ may not exist. However, if A and B are bounded, their domains coincide with Hilbert Space, thereby, obviating such concerns.

Theorem 1 *Consider two operators A and B, therefore:*

$$D(A+B)^* \supset D(A^*+B^*). \qquad (7)$$

An interesting and impressive example for Eq. (7) is considering $A = -B$, it is obvious that $D(A) = D(B)$ and $D(A^*) = D(B^*)$. Now we assume that the domain of operator A is not the whole of Hilbert Space, while the domain of the operator B is whole of Hilbert space. So

$$D(A^*+B^*) = D(A^*) \cap D(B^*) = D(A^*).$$

Moreover, it follows that $D(A+B)^* = 0$, encompasses all of Hilbert Space. It is an exact confirmation of Theorem 1.

Wherein the Hermitian part of an arbitrary operator A may be obtained as below:

$$A^H = \frac{A+A^*}{2}. \quad (8)$$

Now, concerning our discussion in this section, one can write:

$$D(A + A^*)^* \supset D(A^* + A^{**}).$$

Thereby:

$$D(A^H)^* \supset D(A^H). \quad (9)$$

This conclusion again confirms the definition of Hermitian operator (according to the condition $A^{**} = A$).

As previously discussed, a requisite condition for Eq. (7) validity is associated with the boundedness of at least one of the involved operators. However, this criterion does not hold for the position and momentum operators, which are both unbounded. These two operators are exceptions in that Eq. (7) holds for them despite their unbounded nature.

Theorem 2 *Assume the inner product of densely defined A and B operators, then* $(BA)^* \supset A^*B^*$.

For both Theorems, equality is assured by the boundness of one of the operators A or B [7, 8]. In contrast, for Theorem 2, equality would be obtained by another condition that one of the operators should be invertible, and the inverse operator must be bounded [7]. The equality of Theorem 2 can be proved without considering the domain of operators. (Even though paying attention to the domain of operators is considered to prove the equality of this Theorem.)

Assume that, A is an invertible operator.

$$AA^{-1} = I. \quad (10)$$

By multiplying B in both sides we have:

$$BAA^{-1} = B,$$

and by supposing that A^{-1} is bounded one can write:

$$(A^{-1})^*(BA)^* = B^*. \quad (11)$$

According to the fact that $(A^{-1})^* = (A^*)^{-1}$, we conclude:

$$(BA)^* = A^*B^*. \quad (12)$$

Despite what has been mentioned in the latter, none of the mentioned states apply to the equality states of position or momentum operators. Since the mentioned operators are unbounded, the momentum operator is invertible, not bounded. The inverse momentum operator and its domain are:

$$\frac{1}{P} = i\int_{-\infty}^{x} dx\, D\left(\frac{1}{P}\right) = \{\Psi(x) \in L^2(\mathbb{R}, dx) | \int_{-\infty}^{+\infty} \Psi(x')\, dx' = 0.$$

This operator and its generalization in the curved space have been reported in [9].

Now, pay attention to the sum of the two operators. If unbounded operators A and B are Hermitian so the sum of them is also Hermitian. Note that, if both operators were self-adjoint, it would not be obtained that their sum is also self-adjoint [4]. Therefore, considering $A \subset A^*$, and $B \subset B^*$ one can write:

$$(A + B)^* = (A + B) \subset A^* + B^*. \quad (13)$$

Regarding $(A + B)^* \supset A^* + B^*$, (Theorem 1), it is clear that

$$(A + B)^* = A^* + B^*. \quad (14)$$

5 The relationship between creation and annihilation operators

In quantum mechanics, literature, creation and annihilation operators are introduced as complex linear combinations of position and momentum operators, which consist of $a = X + iP$ and $a^\dagger = X - iP$ [1]. These operators are defined with constant coefficients assumed to be one (It should be noted that $*$ symbol is used for an adjoint operator).
For $f \in D(a)$ and $g \in D(a^*)$ we can write:

$$(g, (X + iP)f) = ((X + iP)^* g, f).$$

The left-hand side of the equation will be equal to:

$$(g, Xf) + (g, iPf) = \big((X - iP)g, f\big).$$

In this way, every function g that is in the domain of $a^\dagger$ must also be in the domain of a^*, so it can be concluded:

$$a^\dagger \subset a^*. \quad (15)$$

Similarly, it can be obtained that:

$$a \subset (a^\dagger)^*. \quad (16)$$

It can be concluded that the operators a and $a^\dagger$ are merely a definition and are not generally adjoint to each other.

6 Conclusion

This paper emphasises the crucial role played by the domain of operators in distinguishing between self-adjoint and Hermitian operators. Furthermore, we note that the momentum operator is not self-adjoint due to the existence of certain square-integrable functions that do not vanish at infinity; however, these functions do not belong in the domain

of the momentum operator. Finally, we present our findings on the relationship between creation and annihilation operators in quantum mechanics, which are introduced as being adjoint of each other but have shown not to be generally adjoint of each other.

Reference

1. W. Pauli, *General Principles of Quantum Mechanics* (Springer Verlag, New York, 1980)
2. B. C. Hall, *Quantum Theory For Mathematics* (GTM, Springer, 2013)
3. M. Jafari Matehkolaee, A. Hajimohamadi Fariman, T.Theo. Math. Phy **1**, 1 (2024)
4. K. Schmudgen, *Unbounded self-adjoint operators on Hilbert space* (Springer, 2012).
5. G. Teschi, *Mathematical Methods In Quantum Mechanics, with applications to Schrodinger operators*, 2ed (American Mathematical Society, 2014)
6. M. Jafari Matehkolaee, Pramana-J.Phys. **95**, 131 (2021)
7. J. Weidmann, *Linear operators in Hilbert Spaces* (Springer Verlag, New York, 1980)
8. N. I. Akhiezer, I. M. Glazman, *Theory of Linear operators in Hilbert Spaces* (Pitman, London, Vol I, 1981)
9. M. Jafari Matehkolaee, Pramana J.Phys. **93**, 84 (2019)

TTMP vol 1(2), 2024
doi: 10.30511/TTMP.2024.2025173.1023

Transactions in Theoretical and Mathematical Physics

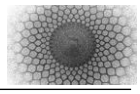

The transition to equilibrium in a system with gravitationally interacting particles. II. Gravitational instability

A. M. Boichenko[1a], M. S. Klenovskii[2]

[1]Institute of Fundamental Problems in Theoretical Physics and Mathematics, Moscow, Russia
[2]University of Chemistry and Technology, Prague, Czech Republic

Received: 20 March 2024 / Accepted: 26 Mai 2024 / Published: 26 Mai 2024

Abstract The distribution function of systems in equilibrium must have the canonical form of the Gibbs distribution. Attempts have been made for more than 100 years to substantiate this behaviour of systems to involve their mechanical behaviour. In other words, it seems that a huge number of particles of the medium, resulting from interaction with each other according to dynamic laws, can explain the statistical behaviour of systems during their transition to equilibrium. Modelling of gravitationally interacting particles is carried out, and it is shown that, in this case, the distribution function does not evolve to the canonical form. Earlier, the same results were obtained for classical Coulomb plasma. On the other hand, such a statistical effect as relaxation is well described by the system's dynamic behaviour, and the simulation data agree with the known theoretical results obtained in various statistical approaches. This article demonstrates that the well-known phenomenon of gravitational instability is also reproduced in the numerical simulation of a system with gravitationally interacting particles.

Keywords: *dynamical behaviour in classical mechanics, substantiation of statistical mechanics, entropy, equilibrium, gravitationally interacting particles.*

1 Introduction

The formulation of the dynamical laws of macroscopic bodies, given by I. Newton, led to successes in quantitatively describing their behaviour. The discovery of the planets of the solar system Neptune (according to the calculations of W.J. Le Verrier and D.C. Adams) and Pluto (according to the calculations of P. Lovell and W.G. Pickering) clearly confirm this. We can predict the positions of the planets for centuries. Methods for describing the mechanical behaviour of systems are constantly being improved [1-12]. However, with increased bodies in the system, predicting their behaviour using Newton's laws becomes much more difficult. Such a prediction becomes impossible for systems with many particles, such as gases, liquids, and solids. In this case, statistical methods of description are used. But we, on the one hand, understand that this huge number of particles must still be described by the laws of dynamics. On the other hand, when trying to do this, we encounter problems that, at first glance, should not arise. The issues of substantiating the statistical description and their connection with the dynamic description have become essential and come to the fore in science since the beginning of the 20th century [13].

If a closed system at a certain moment of time is in a non-equilibrium macroscopic state, then the most probable consequence at subsequent moments of time will be a monotonic increase in the system's entropy. This is the so-called law of increasing entropy or the second law of thermodynamics. It was discovered by R. Clausius, and its statistical justification was given by L. Boltzmann [14-16].

Systems in equilibrium. Conclusions about the increase in entropy in a closed system and the form of the distribution function of systems in equilibrium can be traced in many available monographs. The conclusion that entropy increases (or at least does not change) during an irreversible transition from one equilibrium state to another is proved, for example, in [14] using the postulate that the second kind of perpetuum mobile is impossible. The derivation of the distribution function for closed systems in equilibrium, based on the microcanonical distribution, is contained, for example, in [15]. The distribution function $w(E)$ of systems with energy E in equilibrium depends exponentially on the entropy of the system S,

$$w(E) \propto \exp\left(S(E)\right),$$

[a]boichenko.ifptpm@gmail.com

which is why it is stated that the entropy of a closed system in a state of complete statistical equilibrium has the largest possible value (for a given energy of the system). The form of the distribution function of a system as a function of its entropy is rarely used. Most often, depending on the consideration being carried out, its equivalent representations are used either in the form of a Gibbs distribution (canonical distribution)

$$w(E) \propto \exp(-E/T),$$

where T is the system's temperature or in the form of a Boltzmann distribution. It is generally assumed that when an equilibrium is established in the energy ranges, where the interaction of particles with other particles can be neglected or the interaction of a particle with only the nearest particle can be taken into account, the Gibbs distribution function transforms into the Boltzmann distribution function of particles.

The use of the above-mentioned equilibrium distribution functions has been carried out in consideration of a huge variety of practical problems, so there is no doubt that they are confirmed by all our daily observations. But not everything is as simple as it seems at first glance. The fact is that when considering the world around us as a whole, it is impossible not to notice that with the destruction of some systems, which just corresponds to the growth of the entropy of such systems, the organization or ordering of other systems takes place. The emergence of man is a vivid confirmation of this. However, the processes of structuring and complication of systems lead not to an increase but to a decrease in entropy. To a certain extent, these emerging difficulties have not yet been overcome.

The distribution function of particles is formed due to their interaction during the transition to an equilibrium state. That is why it is natural to assume that the statistical behaviour of the particles must be ultimately described by their dynamic behaviour. It is precisely under the excitation, or when external conditions are changed due to the laws of dynamics, that the interacting particles should line up and redistribute in such a way as to reproduce their distribution function. Everything seems to be logical. However, more than a century of attempts to substantiate this statement did not lead to success. A detailed description of these attempts is given in our previous work [17]. It describes the main milestones on the way to substantiate this position, starting with the Boltzmann hypothesis of a giant fluctuation, involving the explanation of open systems, Gibbs's steps to introduce coarsening of the phase liquid, his introduction of the concept of mixing and further development of this concept in the works of Krylov, Sinai, Kolmogorov and his school, applying Poincare and his followers to questions of regularity and stochasticity of non-integrable systems, attempts to justify the ergodicity of statistical systems, including consideration of ergodicity and quasi-ergodicity in the context of metric transitivity and mixing, consideration of questions about the instability of phase trajectories with the involvement of Lyapunov exponents and ending with the contribution of synergetics to the possible resolution of this issue.

Because the question of substantiating the statistical behaviour of the system by its dynamic behaviour could not be solved, various questions of physics needed to proceed to the justification of various scales (or arrows) of time, among which the main ones were considered, i.e. the thermodynamic scale, cosmological, causal, psychological, and quantum. If we abstract from some details, all these time scales are determined by the thermodynamic scale [17], returning us to the starting point – the need to explain the irreversible growth of entropy in closed mechanical systems.

Why, then, has the justification mentioned above defied the explanation for more than 100 years (it is believed that serious research in this area began after the publication of the review [13])? Aside from considering particle interaction dynamics in a closed system, there must be something else that is not apparent on the surface. It seems that the entropy during the transition to equilibrium should increase. However, as noted above, it can also decrease, which we observe in the example of highly organized systems. However, generally speaking, it should not change. There are rigorously proven theorems on the conservation of entropy in closed mechanical systems, both classical and quantum [18-20]. In addition, the particle motion equations are reversible in time, which should not help explain the irreversible processes of entropy growth.

To clarify this issue, attempts were made to numerically simulate the interaction of particles based on their dynamic behaviour by Newton's laws. This approach has been developed for a long time with various physical issues, i.e. the so-called particle-in-cell simulations [21]. A classical Coulomb plasma was modelled in works [22-27]. Initially, the simulation aimed to refine the rate constant of triple recombination of ions with electrons by ab initio methods. The rate constant was necessary for modelling the kinetics of plasma processes, particularly in questions concerning the theory of plasma lasers and their achievable characteristics [28-36]. However, research very quickly reached the level of fundamental questions of plasma physics and statistical physics. It turned out that the modelled plasma "did not want" to recombine under the known concepts of the recombination process. More precisely, it did not recombine at all. Further, with a more detailed study of this issue, it turned out that the form of the distribution function of plasma particles after establishing equilibrium in numerical simulations is neither Boltzmann nor microcanonical. The

recombination of the simulated plasma began only when the dynamic memory of the system disappeared in one way or another. This was achieved in modelling by introducing various kinds of stochastics; for example, the particle velocities were forcibly rearranged arbitrarily while maintaining their total energy, etc. (for more details, see [17, 22-27]).

In our previous work [17], the simulation was carried out in a system of gravitationally interacting particles. Although the system of gravitationally interacting particles and a system of interacting charged particles seem similar due to the identical behaviour of the interaction force on distance, they have significant distinctions (for more details, see [17]). It turned out that when equilibrium is established, the distribution function of particles, as well as in plasma modelling, is neither Boltzmann nor microcanonical.

So, according to well-known concepts, the form of the distribution function particles that are in equilibrium in closed systems must have the canonical Gibbs form. On the other hand, according to known theorems of mechanics, it cannot have this form since the entropy of a system cannot change and reach its maximum value in equilibrium. The numerical simulations carried out in the above-mentioned works show that the latter case is actually implemented if nothing but the numerical solution of the equations of particle motion according to Newton's laws is used.

In the work [17], numerical methods were used to investigate the distribution function of gravitationally interacting particles and their relaxation time. Even though during the transition to equilibrium, the particle distribution function for the total energy did not take the canonical Gibbs form, the relaxation time, nevertheless, turned out to be in full agreement with the known values obtained by various methods, ranging from simple estimates to its consideration it in the framework of the Fokker-Planck approximation and kinetic description. This paper aims to study gravitational instability within the framework of the same numerical simulation of the behaviour of particles interacting with each other through the law of gravity. This method is described in more detail in our previous work [17].

2 Gravitational instability

In our previous work [17], numerical methods investigated collisional relaxation. The distribution of particles in the space at the initial moment of time was set to be uniform. As is known, the initial uniform distribution of particles is unstable and, under the influence of gravitational forces acting between the particles, breaks up into separate clumps.

For the first time, Jeans formulated and solved the problem of the stability of a uniform distribution of matter [37, 38]. The appearance of celestial bodies and their systems occurs precisely due to the decay of the initial uniform distribution of particles that takes place at the initial stages of the cosmological evolution of the Universe [39-45]. The development of instability occurs due to the competition of two factors: gravity, which tends to collect matter into separate clumps, and pressure, which tends to equalize the resulting non-uniformities.

Let us briefly outline the derivation of the development of instability (see, for example, [40]). The equations of hydrodynamics and gravitation in the Newtonian approximation for an ideal gas have the form:

$$\frac{\partial \rho}{\partial t} + div(\rho\vec{u}) = 0,$$

$$\frac{\partial \vec{u}}{\partial t} + (\vec{u}grad)\vec{u} + \frac{grad(p)}{\rho} + grad(\phi) = 0,$$

$$\Delta\phi = div\big(grad(\phi)\big) = 4\pi G\rho,$$

$$\frac{\partial s}{\partial t} + (\vec{u}grad)s = 0,$$

where ρ is density, $\vec{u}$ is velocity, p is pressure, s is the specific entropy of matter, φ is the gravitational potential, G is the gravitational constant. When considering unstable modes of an undisturbed stationary gas uniformly distributed in space, perturbations are sought in the form of a plane wave superimposed on an undisturbed solution with a frequency ω and a wave vector $\vec{k}$:

$$z = z_0 + \delta(z)\, exp(\,\omega t + i\vec{k}\vec{x}), \qquad (1)$$

where z_0 is the undisturbed value of the magnitude z. As an undisturbed state, we consider a gas at rest ($\vec{u} = 0$) uniformly distributed in space ($\rho = \rho_0 = const$, $S = S_0 = const$, $P = P(\rho_0, S_0) = const$, $grad\ \varphi = 0$).

The resulting system of equations because of substituting the desired quantities of the form (1) has a nontrivial solution for

$$\omega = \pm\sqrt{4\pi G\rho - b^2k^2},$$

where $b^2 = \frac{\partial p}{\partial \rho}$. For long-wave perturbations, the time of increase of perturbations by e times is the value

$$\tau' = \frac{1}{\omega},$$

and in the limit $k \to 0$ ($\lambda \to \infty$) and $\omega \to \sqrt{4\pi G\rho_0}$ is

$$\tau_J = \frac{1}{\sqrt{4\pi G\rho_0}} = \frac{2}{\sqrt{3\pi}}\tau_f, \quad (2)$$

where

$$\tau_f = \sqrt{\frac{3\pi}{16G\rho_0}}, \quad (3)$$

is the free fall time of the point mass to the center of a homogeneous ball of density ρ_0.

Note that random perturbations of a uniform distribution lead to different consequences in the limit of short- and long-waves. In the long-wave limit ($\lambda > \lambda_J$)

$$\lambda_J = \frac{2\pi}{k_J} = b\sqrt{\frac{\pi}{G\rho_0}},$$

the uniformity decays in time τ`, approximately equal to τ_J. In the short-wave limit ($\lambda < \lambda_J$), perturbations lead to the excitation of waves against the background of this distribution.

3 Gravitationally coupled collisionless system

The decay of a uniform distribution of gravitating particles occurs not only due to gravitational instability. Uniform distribution in gravitational systems is also destroyed due to the mechanism of collisionless relaxation (see details in [46-50]). This mechanism is associated with the phase mixing of such a system. When particles move in a stationary potential field ($\frac{\partial \Phi}{\partial t} = 0$), the intrinsic energy of a particle does not depend on time and is equal to

$$\varepsilon = \frac{v^2}{2} + \Phi,$$

where Φ is the potential of the field, and ν is the velocity of the particle, and

$$\frac{d\varepsilon}{dt} = \frac{1}{2}\frac{dv^2}{dt} + \frac{d\Phi}{dt} = \vec{v}\left(\frac{d\vec{v}}{dt} + \nabla\Phi\right) + \frac{\partial\Phi}{\partial t} = 0.$$

.

If the potential changes with time, then the energy of the particles also changes

$$\frac{d\varepsilon}{dt} = \frac{1}{2}\frac{dv^2}{dt} + \frac{d\Phi}{dt} = \vec{v}\left(\frac{d\vec{v}}{dt} + \nabla\Phi\right) + \frac{\partial\Phi}{\partial t} = \frac{\partial\Phi}{\partial t}\Big|_{\vec{x}(t)}.$$

The particles are redistributed in the phase space, and the change in their energy, unlike collisional relaxation, does not depend on the particle's mass. The time of such relaxation in the case of energy fluctuations can be estimated as [46-50]

$$\tau_{LB} \approx \left[\frac{1}{\varepsilon^2}\left(\frac{d\varepsilon}{dt}\right)^2\right]^{\frac{1}{2}}.$$

This time can be associated not with the rate of change in the particle energy but with the rate of change in the potential and the rate of change in the effective radius of the system. Let us consider the spherical collapse of a homogeneous ball of collisionless particles with a total mass of M. It follows from the virial theorem that $2\bar{W}_k \approx -\bar{U}$ or $\bar{U} \approx 2E$, where E is the total energy of the system, W_k is the total kinetic and U is the total potential energy of the system (the bar at the top means the average over time). In this case, given that $E = -\bar{W}_k$, we get $(1/2)mv^2 \approx -(1/2)m\Phi$ or $\varepsilon \approx (1/2)\Phi$, which gives

$$\tau_{LB} \approx \left[\frac{1}{\Phi^2}\left(\frac{d\Phi}{dt}\right)^2\right]^{\frac{1}{2}}.$$

The effective radius of the system of particles can be determined from the condition $U = -\frac{GM^2}{R}$. The angular momentum of system I is proportional to MR^2 with some constant ι^2:

$$I = \iota^2 MR^2.$$

Then, from the nonequilibrium virial theorem [50]

$$\frac{1}{2}\frac{d^2I}{dt^2} = 2W_k + U,$$

we have

$$\iota^2\left[R\frac{d^2R}{dt^2}+\left(\frac{dR}{dt}\right)^2\right]=-\frac{2E}{M}-\frac{GM}{R}=\frac{2|E|}{M}-\frac{GM}{R}.$$

As a result of the occurrence of the $\delta R(t)$ fluctuation, it is possible to write $R(t)=\bar{R}+\delta R(t)$ and, decomposing this differential equation for $R(t)$ near its equilibrium value

$$\bar{R}=-\frac{GM^2}{2E},$$

we obtain an equation for $\delta R(t)$

$$\frac{d^2\delta R}{dt^2}=\frac{GM}{\iota^2\bar{R}^3}\delta R,$$

the perturbation growth index of which is determined by the expression

$$\omega_{LB}^2=\frac{GM}{\iota^2\bar{R}^3}=\frac{4\pi G}{3\iota^2}\bar{\rho},$$

where $\bar{\rho}=\frac{3M}{4\pi\bar{R}^3}$ is the average density of the system. By relating the effective potential to the effective radius of the system

$$\Phi\approx-\frac{GM}{NR},$$

$$\frac{d\Phi}{dt}\approx-\frac{GM}{NR^2}\frac{dR}{dt},$$

where N is the number of particles in the system, we obtain

$$\tau_{LB}\approx\left[\frac{1}{R^2}\left(\frac{dR}{dt}\right)^2\right]^{\frac{1}{2}}\approx\omega_{LB}^{-1}=\sqrt{3}\iota\tau_J=\frac{2\iota}{\pi}\tau_f. \quad (4)$$

That is, the time of collisionless relaxation coincides in order of magnitude with the time of development of gravitational instability (2) and, accordingly, in order of magnitude coincides with the time of free fall (3), i.e. the time of the collapse of a homogeneous cold extended mass into a point. If the initial distribution of particles inside the sphere is uniform, then

$$\iota^2=\frac{2}{5},$$

and the time of collisionless relaxation differs from the time of development of gravitational instability by 10%.

4 Modelling and discussion of the results

Systems with long-range interaction, which include the gravitational and Coulomb interactions, are usually described by the ideality parameter $\delta = \langle U\rangle/\langle W_k\rangle$, (or sometimes by $\gamma \cong \delta^3$) representing the system's mean potential $\langle U\rangle$ energy ratio to its mean kinetic energy $\langle W_k\rangle$. This parameter characterizes the degree of the ideality of the system under consideration. In the ideal case, $\delta << 1$, the consideration of many issues related to the behaviour of such systems is usually greatly simplified.

To consider the instability, a series of calculations was carried out in non-ideal

$\delta >> 1$,

and almost ideal

$\delta \approx 1$,

cases.

In connection with questions of substantiation of the statistical description, it was important to us to be convinced that the system we simulated has gravitational instability. The evolution of the spatial distribution of particles and questions connected to a range of system parameters, with which splitting the system into clumps of particles is possible, were not considered and analyzed.

***Case A* ($\delta \approx 1$).** The calculation parameters were as follows: number of particles was 300, particle mass was 10^{-9} kg, cube edge length was 10^{-6} m, and initial kinetic energy of all particles was the same $W_k = 0.05$ eV. At the initial moment of time, the particles in the cube and the directions of their velocities were distributed uniformly. The absolute values of the particle velocities were set to be the same at the initial moment of time, especially to trace the evolution (see Figs. 1, 2 in [17]) of the particle distribution function in terms of total and kinetic energies (or velocities). Under the conditions listed above, the total potential energy of the system of particles at the initial moment of time was $U = -35.7$ eV (this

corresponds to the mean potential energy of $<U>$ = –0.119 eV). Thus, the absolute value of the ideality parameter at the initial moment of time was $\delta \approx 2.4$, and the time for the development of gravitational instability (and collisionless relaxation) according to (2) and (4) should be 0.063 s. This value is in good agreement with the results of numerical calculations. Indeed, the initial distribution of particles begins to deform approximately from 10^{-2} s, and by 10^{-1} s concentrations for different groups of particles change by a factor of two or more times (Fig. 1). Recall that the distribution of particles in kinetic energy is almost completely formed only by 1-2 s; it has the form of a Maxwell distribution with a temperature approximately equal to 0.08 eV (see Figs. 1, 2 in [17]). At the initial moment of time, it is impossible to talk about the temperature of particles, since all particles have the same kinetic energy. It makes sense to talk about temperature only at the moment of relaxation time (about 2 s, see [17] for more details), at which the ideality parameter is already $\delta \approx 1.66$.

The relaxation time obtained in the numerical simulations [17] coincides well with the time obtained in the theoretical consideration of relaxation processes. However, the question arises: until when should the calculations be performed to ensure the relaxation process is over? It may turn out that the system will continue to evolve. For example, the relaxation time in numerical experiments can be significantly longer than τ, and then on time scales of the order of τ, the changes in the distribution function are simply almost imperceptible. In this case, the virial theorem comes to the rescue. In systems with gravitational interaction, the average absolute value of δ should be 2 if particles occupy a limited volume. The absolute value of parameter δ goes to the value of 2 by about 0.5 s and then does not change, i.e. it means that the system turns to the stationary state.

It seemed it is possible to object that nothing prevents to vary $<U>$ and $<W_k>$ so that the statement of the virial theorem [51] remains true

$$2 < W_k >= k < U >= - < U >, \qquad (5)$$

($k = -1$ for gravitational interaction). However, it not so. In view of that

$$< W_k > + < U >= < E >= E,$$

we have

$$< U >= \frac{2}{k+2} E = 2E,$$

$$< W_k >= \frac{k}{k+2} E = -E,$$

whence it is visible, that if $<U>$ and $<W_k>$ are in accordance with (5), they already further cannot vary.

Note also, that if we remove the walls in the calculations, then the particles continue to move in a compact region without escaping, despite the absence of any boundaries, and the absolute value of parameter δ goes to the value of 2 also by about 0.5 s and then does not change. Consequently, there will be no further redistribution of the values of the kinetic and potential energies in the system.

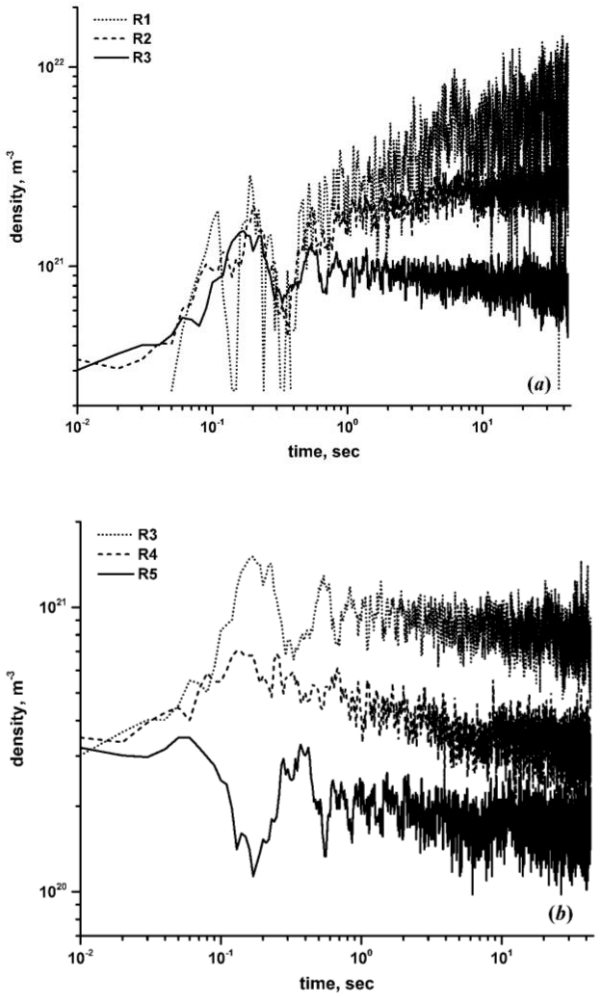

Fig. 1. Dependencies of particle density on time. The particles (300 particles each of mass 10^{-9} kg) are initially uniformly distributed in a cube with the edge of $a = 10^{-6}$ m. The designation on the graph R_i corresponds to the density of particles in a spherical layer from $0.5 \cdot a \cdot (i-1)/n$ to $0.5 \cdot a \cdot (i)/n$, where $n = 5$ is the total number of spatial partitioning layers and $i = 1, ..., n$ is the number of a specific layer.

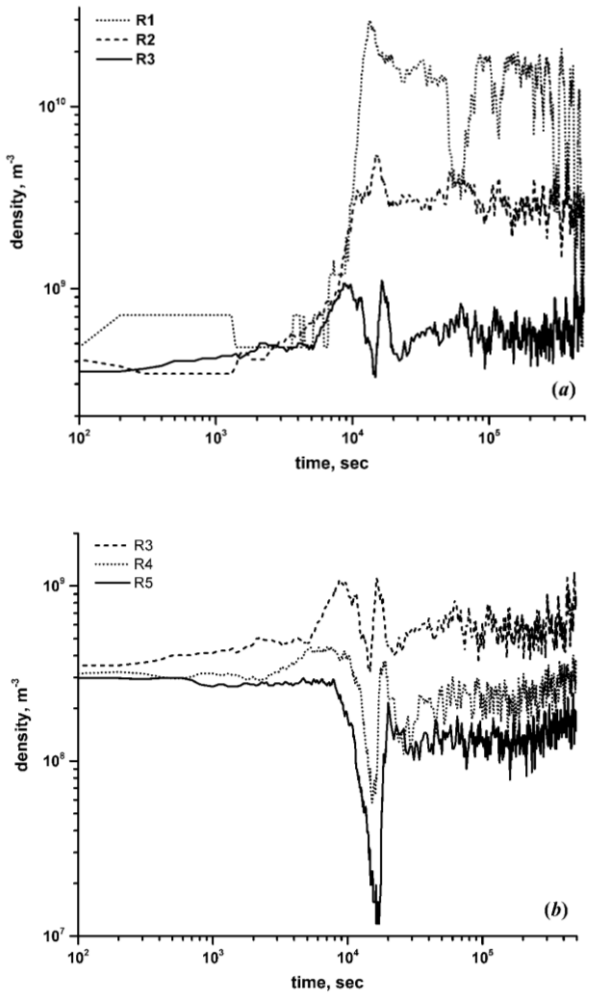

Fig. 2. Dependencies of particle density on time. The particles (300 particles each of mass 10^{-7} kg) are initially uniformly distributed in a cube with the edge of $a = 10^{-2}$ m. The designation on the graph R_i corresponds to the density of particles in a spherical layer from $0.5 \cdot a \cdot (i-1)/n$ to $0.5 \cdot a \cdot (i)/n$, where $n = 5$, $i = 1, ..., n$.

***Case B* (δ >> 1).** The calculation parameters were as follows: number of particles was 300; particle mass was 10^{-7} kg; temperature of particles was $T = 10^{-2}$ eV (originally Maxwell distribution); cube edge length was 10^{-2} m. At the initial moment of time, the particles in the cube and the directions of their velocities were distributed uniformly. In this case, the absolute velocities of the particles at the initial moment of time were not set the same. However, there are no qualitatively significant differences in the evolution (see Figs. 3, 4 in [17]) of the particle distribution function in terms of total and kinetic energies (or velocities) compared to the previous case *A*. Under the above conditions, the total potential energy of the particle system at the initial moment of time was $U = -36.2$ eV, so the absolute value of the ideality parameter at the initial moment of time was $\delta \approx 8.04$ (if we take into account that $< W_k > = 1.5T$). The time for the development of gravitational instability (and collisionless relaxation), according to (2) and (4), should be $6.3 \cdot 10^3$ s. This value is in good agreement with the results of numerical calculations. Indeed, the initial distribution of particles begins to deform approximately starting from $4 \cdot 10^3$ s and by 10^4 s, concentrations for different groups of particles vary by a factor of two or more times (Fig. 2). Recall that the kinetic energy distribution of particles is almost completely formed by $1.5 \cdot 10^4$ - $2 \cdot 10^4$ s; it has the form of a Maxwellian distribution with a temperature approximately equal to 0.12 eV (see Figs. 3, 4 in [17]).

The relaxation time obtained in the numerical simulations [17] coincides well with the time obtained in the theoretical consideration of relaxation processes. Just as in the case *A*, the average absolute value of δ should be 2. Note, that if we remove (or not remove) the walls in the calculations, then this value goes to the value of 2 to about 25000 s and then does not change. Therefore, there will be no further redistribution of the values of the kinetic and potential energies in the system. Just as in the case *A*, (if walls were removed) the particles continue to move in a limited area without escaping.

5 Conclusions

Numerical simulation of the behaviour of classical particles interacting gravitationally with each other was carried out. The conducted modelling is directly related to the question of the possibility of substantiating the statistical behaviour of classical mechanical systems based on their mechanical behaviour. The cases with the ratio of the potential energy to the kinetic energy (ideality parameter) of $\delta \geq 1$ at the initial conditions were considered. The main results obtained in the work can be summarized as follows.

1. The decay of a homogeneous distribution of gravitationally interacting particles occurs due to the development of gravitational instability. The time of development of this instability is well known. It was obtained using the Jeans approach and in subsequent works by various authors. The collisionless relaxation mechanism of gravitational systems can also contribute to the collapsing of a homogeneous particle distribution. The duration of both mechanisms is approximately the same and coincides in magnitude with the time obtained in the numerical simulation carried out in this paper.

2. The relaxation time of the system obtained based on the numerical simulation [17] is also in good agreement with the relaxation time obtained in a large number of studies using various approximations.

3. However, the purely gravitational interaction of particles does not lead to the formation of Boltzmann form's particle energy distribution function in the region

of large magnitude negative energies [17]. Such behaviour must occur in accordance with the known theorems when the system approaches its equilibrium. Almost more than a century of attempts have been made to justify such a transition and to concordance the statistical and mechanical approaches in such a transition.

4. On the other hand, such behaviour should not also occur in accordance with other known theorems. In the language of entropy, the transition to the equilibrium corresponds to the system's transition to the state with the highest possible entropy. However, the well-known entropy conservation theorems for mechanical closed systems in both classical and quantum cases prevent such a transition since the entropy of such systems cannot change.

5. Thus, the current work demonstrates another example of a system in which, when approaching its equilibrium, the distribution function does not take the canonical form if the system does not involve any other factors besides its mechanical behaviour. Earlier, a similar result was demonstrated in the example of a classical Coulomb plasma.

6. Thus, it is generally impossible to justify the transition of the distribution function of a closed system in equilibrium to the canonical Gibbs distribution only based on its mechanical behaviour for systems with long-range Coulomb or gravitational interactions. For such a justification, it is necessary to consider the presence of other processes in the system in addition to only the mechanical interaction of particles with each other. For example, the system must have a stochastiser in one form or another, which will remove the ban on changing the entropy of closed systems imposed by the well-known entropy conservation theorems.

References

1. C. G. J. Jacobi, *Vorlesungen uber dynamik* (Open Library, 1866)
2. G. R. Kirchhhoff, *Vorlesungen uber mathematische physik. Mechanik* (Open Library, 1877)
3. Poincare. *Les Methodes Nouvelles de la Mecanique Celeste* (Open Library, 1899)
4. E. T. Whittaker. *A treatise on the analytical dynamics of particles and rigid bodies with an introduction to the problem of three bodies* (Cambridge University Press., 1927)
5. A. Sommerfeld, *Mechanik* (Zweite, Revidierte Auflage, 1944)
6. A. I. Lurie, *Analytical mechanics* (Moscow Fizmatlit, 1961 - in Russian)
7. F. R. Gantmacher, *Lectures on analytical mechanics*. (Moscow Fizmatlit, 2001 - in Russian)
8. C. L. Siegel, J. K. Moser., *Lectures on celestial mechanics* (Springer-Verlag Berlin, Heidelberg New York, 1971)
9. A. Katok, B. Hasselblat, *Introduction to the modern theory of dynamical systems* (Cambridge University Press. , 1998)
10. V. I. Arnold, V. V. Kozlov, A. I. Neustadt, *Mathematical aspects of classical and celestial mechanics* (Moscow: Editorial URSS, 2002 - in Russian)
11. A. M. Boichenko, Bull. Lebedev Phy. Inst. **35**, 7 (2008)
12. A. M. Boichenko, Astrophy. **47**, 1 (2004).
13. P. Erenfest, T. Erenfest, *Bergriffische der statistischen Auffassung in der Mechanik* (Enzyklopadie der mathematischen Wissenschaften, Leipzig, 1911)
14. M. A. Leontovich, *Introduction to thermodynamics* (Leningrad State Publishing House of Technical and Theoretical Literature, 1952 - in Russian)
15. L. D. Landau, E. M. Livshits *Statistical physics* (Moscow: Science, 1964 - in Russian)
16. S. Carnot, W. Thomson (Lord Kelvin), R. Clausius, L. Boltzmann, M. Smolukhovsky, *The second beginning of Thermodynamics*. (Moscow: URSS, 2007 - in Russian)
17. A. M. Boichenko, M.S. Klenovskii, Phy. Sc. Int. J. **25**, 6 (2021)
18. N. N. Bogoljubov, N. N. Jr. Bogoljubov, *Introduction to the quantum statistical mechanics* (Moscow: Science, 1984 - in Russian)
19. J. E. Mayer, M. G. Mayer, *Statistical mechanics* (John Wiley & Sons, 1977)
20. A. M. Boichenko, Quan. Computers and Computing **5,** 1 (2005)
21. R. W. Hockney, J. W. Eastwood *Computer simulation using particles* (McGraw Hill, 1981)
22. S. A. Maiorov, A. N. Tkachev, S. I. Yakovlenko Trudy IOFAN **40**. (1992) (in Russian)
23. S. A. Maiorov, A. N. Tkachev, S. I. Yakovlenko, Usp. Fiz. Nauk. **164**, 3 (1994) (in Russian)
24. S. I. Yakovlenko, Phys. of Vibrations **6**, 4 (1998)
25. A. N. Tkachev, S. I. Yakovlenko, Izv.VUZov. Phy. **41**, 1 (1998) (in Russian)
26. A. N. Tkachev, S. I. Yakovlenko, Las. Phys. **12**, 9 (2002)
27. A. M. Boichenko, S.I. Yakovlenko, Quant. Electr. **24**, 3 (1994)
28. L. I. Gudzenko, S. I. Yakovlenko, *Plasma lasers* (Moscow: Atomizdat, 1978 - in Russian)
29. S. I. Yakovlenko, Las. Phys. **1**, 6 (1991)
30. A. M. Boichenko, V. F. Tarasenko, S. I. Yakovlenko, Las. Phys. **10**, 6 (2000)

31. S. I. Yakovlenko, *Encyclopedia of low-temperature plasma*. (Nauka MAIK Interperiodica, 2000 - in Russian)
32. S. I. Yakovlenko, *Encyclopedia of low-temperature plasma, Series B* (Moscow: Fizmatlit, 2005 - in Russian)
33. A. M. Boichenko, V. F. Tarasenko, S. I. Yakovlenko, *Encyclopedia of low-temperature plasma, Series B* (Moscow: Fizmatlit, 2005 - in Russian)
34. S. I. Yakovlenko, *Gas Lasers* (CRC Press, Taylor & Francis 2007)
35. A. M. Boichenko, A. N. Panchenko, V. F. Tarasenko, A. N. Tkachev, S. I. Yakovlenko, N. A. Panchenko, *Gas and plasma lasers* (Tomsk: STT Publishing, 2017 - in Russian)
36. A. M. Boichenko, *Lamp Emission Sources. Theoretical description* (Academic Publishing, 2018 - in Russian)
37. J. H. Jeans, Royal Soc. Lon. Phil. Trans. Ser. A. **199** (1902)
38. J. H. Jeans, *Astronomy and Cosmology* (Cambridge Univ. Press, 1969)
39. I. R. King, *An introduction to classical stellar dynamics* (University Science Books, 2000)
40. Y. B. Zel'dovich, I. D. Novikov, *Structure and evolution of the universe* (Moscow: Science, 1975 - in Russian)
41. G. G. Boyd, A. D.Chernin, M. J. Valtonen. *Cosmology, Foundations and Frontiers* (Moscow, URSS, KomKniga, 2007)
42. S. Weinberg, *Cosmology* (Oxford University Press, 2008)
43. D. S. Gorbunov, V. A. Rubakov, *Introduction to the theory of the earlier universe. Cosmological perturbations. Inflation theory, V.2* (Moscow, URSS, Krasand, 2010 - in Russian)
44. V. N. Lukash, V. E. Mikheeva, A. M. Malinovsky, Usp. Fiz. Nauk. **181**, 10 (2011 - in Russian)
45. V. E. Fortov, *Physics of high-density energies* (Moscow: Fizmatlit, 2012 - in Russian)
46. D. Lynden-Bell, Mon. Not. Royal Astr. Soc. **136** (1967)
47. F. H. Shu, Astr. Phys. J. **225** (1978)
48. T. K. Nakamura, Astr. Phys. J. **531** (2000)
49. L. Arad, D. Lynden-Bell, Mon. Not. Royal Astr. Soc. **361** (2005)
50. G. V. Vereshchagin, A. G. Aksenov, *Relativistic kinetic theory with applications in astrophysics and cosmology* (Moscow: Science, 2018 - in Russian)
51. L. D. Landau, E. M. Livshits, *Mechanics* (Moscow: Science, 1965 - in Russian)

TTMP vol 1(2), 2024
doi: 10.30511/TTMP.2024.2027905.1026

Transactions in Theoretical and Mathematical Physics

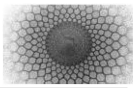

Study of all possible interactions in the quantum three-body problem with Calogero-Sutherland Hamiltonian

A. Latifi[a], **H. Rahmati**

[1]Department of Mechanics, Faculty of Physics, Qom University of Technology, Qom, Iran

Received: 01 May 2024 / Accepted: 30 May 2024 / Published: 30 May 2024

Abstract In the quantum three-body problem, There are three possible models: 1. Each particle interacts independently with the two others, forming three interacting pairs. Pairwise interactions refer to this model. 2. Each particle interacts with the centre of mass of the two others, called the pure three-body interaction. 3. Each particle interacts with the centre of mass of the two others. This kind of interaction is called the pure three-body interaction. 3. Each particle interacts simultaneously with the two others and with the centre of mass of the two others. This latest is called the full-three-body interaction, which combines pairwise and pure three-body interactions. Therefore, knowing which of these models prevails in a given physical context is essential. In this paper, we choose the integrable Calogero Sutherland Hamiltonian, and we explicitly write the wave functions of the ground states in each of these modellings for three fermions and three bosons on a ring. These wave functions reveal regions of the null probability of the presence of particles. This theoretical distribution of probability is to be compared with observations to discover which of these models prevails in the observed physical context. As a physical context, we suggest cold atoms' ring-shaped optical lattices. In addition, we clarify several points about the relation between trigonometric and inverse square interactions on a line and a ring.

Keywords: *Three-body quantum Problem; two-body interactions; Calogero-Sutherland Hamiltonian; three-body interactions; ring-shaped optical lattices*

[a]latifi@qut.ac.ir

1 Introduction

In recent decades, significant efforts have been made to consider convenient Hamiltonians to describe material properties properly. In this context, one of the efficient procedures is, for a given potential, to classify the way particles interact as a many-body system. Namely, pure two-body interactions, two and three-body interactions simultaneously, and two or three-body interactions separately. [1]. Among recent works using this approach, one can mention [2, 3] based on two-body interactions and [4, 5] taking into account three-body interaction, for various potentials.

In parallel, solvable models often provide insights to initiate further approximations or numerical investigations. In the case of many-body quantum systems, the knowledge of the ground state is of great importance, not only because it determines the complete structure of the spectrum [6, 7], but also, as we are going to show in the case of three-body quantum systems, it reveals essential correlations among particles. For this reason, in the particular case of three-body quantum systems, many efforts have been made, in the particular case of the solvable model of Calogero-Sutherland (CS), to generalize the pairwise interactions, to pure three-body and full three-body interactions [8–12]. Let us remember that the pure three-body interactions are the interaction between each particle of the system with the centre-of-mass of the two others. The full three-body interactions are the simultaneous two and three-body interactions.

In this paper, we consider the one-dimensional CS model, which, beyond its solvability, plays an important role in various domains of physics [13, 14] as different as the physics of black holes[15] or the quantum Hall effects [16]. In the case of three identical particles on a

ring described by the CS model, we give each model's explicit wave functions for fermions and bosons: full three-body interactions, pairwise interactions and pure three-body interactions.

Although experimental setups to highlight inverse square or trigonometric interactions are a real challenge for experimentalists, various experiments have been realized in the context of cold atoms ring-shaped optical lattices [17], some others are suggested to be realized [18], and a global review can be found in [19]. Based on our present study, the experimental observation of particles' probability of presence can inform which model best describes the system correctly and accurately: the full three-body interactions or the pure pairwise or triplet interactions.

The paper is organized as follows: In section (2), we make some rigorous considerations about the relation between spatial and angular coordinates of particles on a line and on a ring, as well as some essential clarification on the relation between inverse square and trigonometric interactions in the case of the three-body problem. In section (3), we briefly recall the method of obtaining the wave function of the full trigonometric C-S Hamiltonian. In section (4), we write the system's wave function for full three-body interactions for fermions and bosons. We obtain all the system's forbidden configurations by solving the null density probability equation. In Sections (5) and (6), the same work is done for pure three-body and pairwise interactions, respectively. In section (7), we conclude and discuss the outlooks.

2 Rigorous considerations

The pioneer study [20] reports on the N-body quantum system online in pairwise interaction with an inverse square potential $V(r) = g/r^2$, where r represents the distance between two particles and g is a real constant. This work has been generalized to the periodic case for N particles [21], by considering N particles on a ring with a circumference equal to L, where the following identity is introduced:

$$V(r) = \frac{g}{r^2} = g\sum_{-\infty}^{+\infty}(r+nL)^{-2} = \frac{g\pi^2}{L^2}\left[\sin\left(\frac{\pi r}{L}\right)\right]^{-2}. \quad (1)$$

Eq. (1) can be justified as follows: at the first stage, the periodicity is obtained by placing after the first pair of particles r apart, N particles at regular distances L apart from each other. Hence, we have N pairwise interactions between the first and the second particle r apart, the first and the third particle $r+L$ apart, the first and the fourth particle $r+2L$ apart, etc. In the second stage, the line is wrapped into a circle. Consequently, the distances in the trigonometric form of the potential are angular. The relation between angular and linear distances is clarified in Eq. (3). However, in the thermodynamics limit, the equalities of Eq. (1) are valid rigorously.

The particular case of three particles *on line*, has been considered in [8] and [22] where polar coordinates are defined to study the problem with the potential $V(r) = g/r^2$.

Later, the interaction of three particles via three body trigonometric potential [10] was considered, and in a more abstract approach, interactions of type r^{-2} and $\left[\sin\left(\frac{\pi r}{L}\right)\right]^{-2}$ were studied as two distinguished cases, and were classified in two distinguishable mathematical categories [9][11].

In this section, we intend to dissipate two ambiguities. First, as mentioned above, the trigonometric potential is only valid in the thermodynamics limit for many particles. Therefore, a legitimate question is how rigorously one can consider a three-body trigonometric potential, far from the thermodynamics limit, and still use Eq. (1). The second point, directly related to the first, concerns the relation between trigonometric and inverse square interactions.

The standard way to justify using the trigonometric interaction for three particles is to consider the limit as the ring's radius grows and tell that the trigonometric and inverse square interactions coincide in this limit.

We intend to go beyond this standard justification and clarify these points without considering the ring's radius limit. To this end, let $\overline{x_ix_j}$, be the distance of the straight line between particles labelled i and j, with $i,j = 1,2,3$, and $\widehat{x_ix_j}$, the length of the arc between particles i and j, on the ring. It is easy to see that $\overline{x_ix_j} = 2Ox_i\sin(\theta/2)$, where θ is the angle between the two radius Ox_i and Ox_j of the ring, (see Figure 1). Using fundamental trigonometric relations, we have

$$\overline{x_ix_j} = \frac{L}{\pi}\sin\left(\frac{\pi}{L}\,\widehat{x_ix_j}\right). \quad (2)$$

It follows,

$$\frac{g\pi^2}{L^2}\frac{1}{\left[\sin\left(\frac{\pi}{L}(\widehat{x_ix_j})\right)\right]^2} = \frac{g}{[\overline{x_ix_j}]^2}. \quad (3)$$

Hence, taking into account that $r = a^{-1}\sin[a(x_i - x_j)]$, where $r = \overline{x_ix_j}$, and $a = \pi/L$, Eq. (3) shows that the trigonometric potential and the inverse square potential represent both, the same type of interactions, in the sense that, the strength of the potential, is proportional to the inverse of the square of the distance

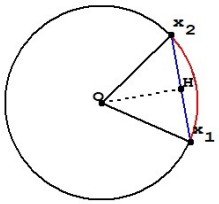

Fig. 1 The relation between the distance $\overline{x_i x_j}$ and the length of the arc $\widehat{x_i x_j}$ leading to Eq. (3) can be seen in this panel.

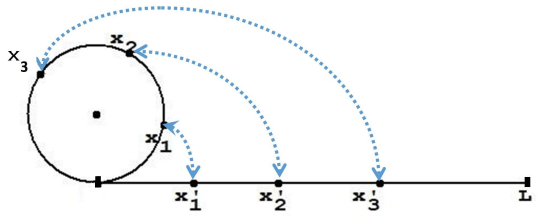

Fig. 2 The case of particles on a ring is *not* a simple winding of the segment of length L on a circle with the same circumference, but a mapping which *does not conserve the length.*

between particles. Consequently, trigonometric and inverse square potentials can be mapped from one to the other. However, we must remember that this mapping is not isometric and does not conserve the length. Indeed, as illustrated in Figure 2, the distance of the arc $\widehat{x_i x_j} = \overline{x'_i x'_j} \neq \overline{x_i x_j}$, $i,j = 1,2,3$. This is the fundamental care that must be taken when using the trigonometric interaction far from the thermodynamic limit or without considering a ring with an infinitely large radius.

3 Transformation of CS Hamiltonian into Laplace-Beltrami Hamiltonian

We consider the full trigonometric Hamiltonian with full three-body interactions of CS type for three identical distinguishable fermions with mass m on a ring. This Hamiltonian reads [12]:

$$H^{full} = \frac{-\hbar^2}{2m}\sum_{i=1}^{3}\left(\frac{\partial}{\partial x_i}\right)^2 + \frac{\hbar^2}{m}\nu(\nu-1)a^2\sum_{\substack{i,j=1\\ i\neq j}}\frac{1}{\sin^2[a(x_i-x_j)]} + \frac{\hbar^2}{m}\mu(\mu-1)a^2\sum_{\substack{i,j,k=1\\ i\neq j\neq k}}\frac{1}{\sin^2[a(x_i+x_j-2x_k)]}, \quad (4)$$

where $a(x_i - x_j)$ is the angular distance between particles, while $a(x_i + x_j - 2x_k)$ is the angular distance between one of the particles and the centre-of-mass of the two others. $0 < \mu < 1$ and $0 < \nu < 1$ are real coefficients, $\hbar$ is the Planck constant, and a is a constant homogeneous to the inverse of length, namely $a = \pi/L$, where L is the circumference of the ring.

Notice that the pairwise interactions vanish for $\nu = 0$ or $\nu = 1$. The Hamiltonian (4) coincides with the Sutherland Hamiltonian [21], whilst the three-body interactions vanish for $\mu = 0$ or $\mu = 1$, in which case, the Hamiltonian in Eq. (4) covers the three-body inverse-square potential on a line studied in [8]. Also, notice that the constraints $0 < \mu < 1$ and $0 < \nu < 1$ ensure the system's stability. Indeed, within these ranges of values, the interactions are attractive. Otherwise, they are repulsive and cause the instability of the system.

The method to find the wave function of the Hamiltonian (4) is exposed in [12] and consist of separating the Hamiltonian (4) as the sum of H_{CM}^{full} and H_{rel}^{full}, the Hamiltonian of the centre-of-mass and the relative Hamiltonian, respectively. Then, the following change of variables:

$$z_j = \exp[2ia(R - x_{kl})], \quad (5)$$

where $x_{kl} = x_k - x_l$, $k,l = 1,2,3$ and $R = \frac{1}{3}(x_1 + x_2 + x_3)$ transform H_{CM}^{full} and H_{rel}^{full} into $\widetilde{H}_{CM}^{full}$ and $\widetilde{H}_{rel}^{full}$, as follows:

$$\widetilde{H}_{cm}^{full} = \frac{4}{3}\frac{\hbar^2 a^2}{m}\left(\sum_{j=1}^{3} z_j \frac{\partial}{\partial_{z_j}}\right)^2, \quad (6)$$

$$\widetilde{H}_{rel}^{full} = 6\frac{\hbar^2 a^2}{m}\left[\sum_{j=1}^{3}\left(z_j\frac{\partial}{\partial_{z_j}}\right)^2 + (\nu+\mu)\sum_{\substack{j,k=1\\ j\neq k}}^{3}\frac{z_j+z_k}{z_j-z_k}\left(z_j\frac{\partial}{\partial_{z_j}}\right)\right]. \quad (7)$$

Notice that $\widetilde{H}_{rel}^{full}$ expressed in Eq. (7) is the so-called Laplace-Beltrami Hamiltonian.

4 Forbidden configurations in the case of full three-body interactions

4.1 three identical distinguishable fermions with full three-body interactions

The eigenfunction of $\widetilde{H}_{rel}^{full}$ for three fermions reads [12]:

$$\psi_{rel}^{full,fermions}(z_j) = J_{\{2,1,0\}}^{(\mu+\nu)^{-1}}(z_1,z_2,z_3) \times \prod_{\substack{j,k=1 \\ j\neq k}}^{3}(z_j-z_k)^{(\nu+\mu)}, \quad (8)$$

where

$$J_{\{2,1,0\}}^{(\mu+\nu)^{-1}}(z_1,z_2,z_3) = z_1^2z_2+z_2^2z_1+z_1^2z_3+z_3^2z_1+z_2^2z_3+z_3^2z_2. \quad (9)$$

$J_{\{2,1,0\}}^{(\mu+\nu)^{-1}}$ is the Jack polynomial for the partition $\{2,1,0\}$ which is the only possible partition for three fermions in the Fock space. For more details, see [12] and related references therein. Hence, in terms of the variable z_j, Eq. (8) reads

$$\psi_{rel}^{full,fermions}(z_1,z_2,z_3) = \left(z_1^2z_2+z_1^2z_3+z_2^2z_1+z_2^2z_3+z_3^2z_1+z_3^2z_2\right) \times [(z_1-z_2)(z_2-z_3)(z_3-z_1)]^{(\nu+\mu)}. \quad (10)$$

Back to the initial coordinates x_1, x_2 and x_3 by using Eq. (5) and, relative distances $x_{ij}=x_i-x_j$, $i,j=1,2,3$, Eq. (10) becomes:

$$\begin{aligned}&\psi_{rel}^{full,fermions}\\ &= \left[e^{-4iax_{23}-2iax_{31}}+e^{-4iax_{23}-2iax_{12}}+e^{-4iax_{31}-2iax_{23}}\right.\\ &\left.+e^{-4iax_{31}-2iax_{12}}+e^{-4iax_{12}-2iax_{23}}+e^{-4iax_{12}-2iax_{31}}\right]\\ &\times\left[(e^{-2iax_{23}}-e^{-2iax_{31}})(e^{-2iax_{31}}-e^{-2iax_{12}})\right.\\ &\left.\times(e^{-2iax_{12}}-e^{-2iax_{23}})\right]^{(\nu+\mu)} \quad (11)\end{aligned}$$

It is worth noticing that μ and ν does not appear separately in Eq. (11), but appears only as the sum $\mu+\nu$. Therefore, the probability density of particles depends on $\mu+\nu$. As seen in Eq. (4), ν and μ determine the strength of pure two and pure three-body interactions, respectively. Consequently, it is impossible to distinguish the strength of each interaction separately.

Straight forward calculations yield the density of probability $|\psi_{fermion}|^2$ as follows:

$$\begin{aligned}|\psi_{rel}^{full,fermions}|^2 =& 2^{(1+3\nu+3\mu)}\left[3+2\cos 2a(x_{21}+x_{31})\right.\\ &+2\cos 2a(x_{13}+x_{23})2\cos 2a(x_{12}+x_{32})\\ &+\cos 4a(x_{12}+x_{32})+\cos 4a(x_{23}+x_{13})\\ &+\cos 4a(x_{31}+x_{21})+2\cos 6ax_{12}\\ &\left.+2\cos 6ax_{23}+2\cos 6ax_{31}\right]\\ &\times[(1-\cos 2ax_{12})(1-\cos 2ax_{23})\\ &\times(1-\cos 2ax_{31})]^{(\nu+\mu)} \quad (12)\end{aligned}$$

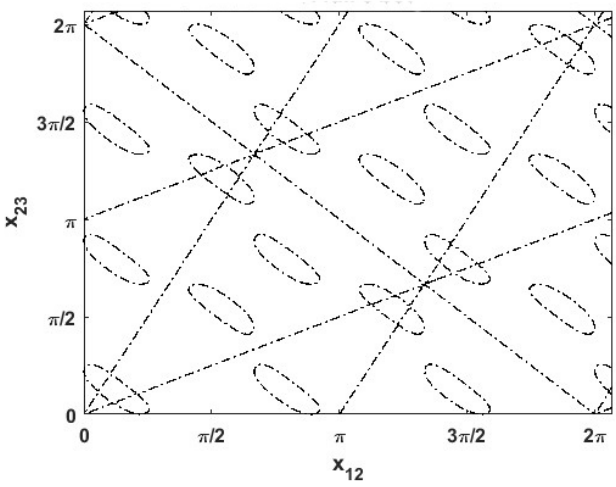

Fig. 3 The configurations with null probability for $a=0.5$, in the case of three identical distinguishable fermions with the full 3-body interactions. x_{12} is the relative distance between particles labelled 1 and 2 and, x_{23} is the relative distance between particles labelled 2 and 3.

The configurations with null probability corresponding to $|\psi|^2=0$ for $a=0.5$, are shown in Figure 3. Notice that $a=0.5$ corresponds to the circumference $L=2\pi$.

Figure 3 is a superposition of lines and ellipses. Any point of these lines or ellipses constitutes a forbidden configuration for fermions on the ring. For instance, the equation of one of these lines reads $x_{23}=\pi x_{12}$. Therefore $x_{12}=\frac{\pi}{2}$ and $x_{23}=\frac{\pi^2}{2}$ constitute a forbidden configuration. i.e. the angular distance $\widehat{x_1x_2}=45$ and $\widehat{x_2x_3}\approx 103$ degrees is one of the infinite number of forbidden configurations in this case.

4.2 three identical distinguishable bosons with full three-body interactions

The suitable partition for three bosons is $\{3,0,0\}$. The Jack polynomial for this partition reads

$$J_{\{3,0,0\}}^{(\mu+\nu)^{-1}}(z_1,z_2,z_3) = 2(z_1^3+z_2^3+z_3^3). \quad (13)$$

Therefore, the eigenfunctions of $\widetilde{H}_{rel}^{full}$ for three bosons reads

$$\psi_{rel}^{full,boson}(z_j) = (z_1^3+z_2^3+z_3^3+z_1^3+z_2^3+z_3^3) \times[(z_1-z_2)(z_2-z_3)(z_3-z_1)]^{(\nu+\mu)}. \quad (14)$$

Back to the initial coordinates x_1, x_2 and x_3 by using Eq. (5) and, relative distances $x_{ij}=x_i-x_j$, $i,j=1,2,3$, Eq. (14) yields

After straight forward calculations, we obtain the density of probability $|\psi_{rel}^{full,boson}|^2$ as follows:

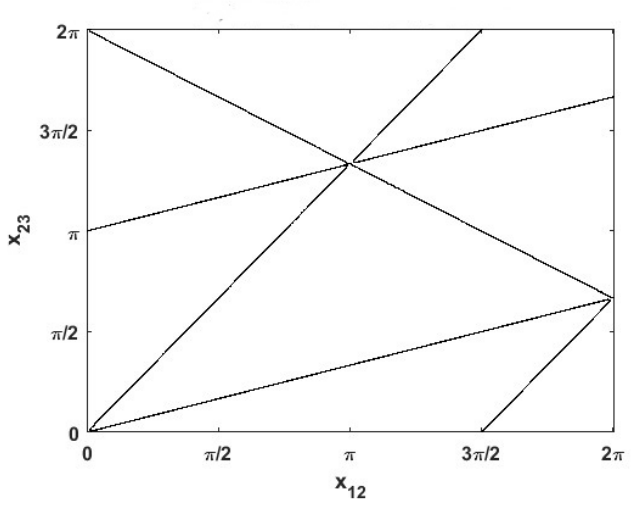

Fig. 4 The configurations with null probability for $a = 0.5$, in the case of three identical distinguishable bosons with the full 3-body interactions. x_{12} is the relative distance between particles labelled 1 and 2 and, x_{23} is the relative distance between particles labelled 2 and 3.

$$
\begin{aligned}
|\psi_{rel}^{full,boson}|^2 = 2^{2+3\nu+3\mu}[3 &+ 2\cos(6a(x_{12}+x_{32})) \\
&+ 2\cos(6a(x_{12}+x_{13})) + 2\cos(6a(x_{23}+x_{13}))] \\
&\times [(1-\cos 2ax_{12})(1-\cos 2ax_{23}) \\
&\times (1-\cos 2ax_{31})]^{(\nu+\mu)}. \qquad (15)
\end{aligned}
$$

$$
\begin{aligned}
\psi_{rel}^{full,boson} =& 2\left[e^{-6iax_{12}} + e^{-6iax_{23}} + e^{-6iax_{31}}\right] \\
&\times \left[(e^{-2iax_{23}} - e^{-2iax_{31}})(e^{-2iax_{31}} - e^{-2iax_{12}})\right. \\
&\times \left.(e^{-2iax_{12}} - e^{-2iax_{23}})\right]^{(\nu+\mu)}. \qquad (16)
\end{aligned}
$$

The null probability configurations are obtained by letting $|\psi_{rel}^{full,boson}|^2 = 0$. These configurations for $a = 0.5$, are plotted in Figure 4. The lines of Figure 4 are similar to those of Figure 3. These two figures differ only due to the ellipses of Figure 3 that are not present in Figure 4.

5 Forbidden configurations in the case of pure three body interactions

In the case of pure three body interactions, by setting $\nu = 0$ in (4), the Hamiltonian of the system reads:

$$
\begin{aligned}
H^{(pure-3body)} =& \frac{-\hbar^2}{2m}\sum_{i=1}^{3}\left(\frac{\partial}{\partial x_i}\right)^2 \\
&+ \frac{\hbar^2}{m}\mu(\mu-1)a^2 \sum_{\substack{i,j,k=1 \\ i\neq j\neq k}} \frac{1}{\sin^2[a(x_i+x_j-2x_k)]}, \qquad (17)
\end{aligned}
$$

the Hamiltonian (17) is the sum of system's Center of Mass Hamiltonian $H_{CM}^{(pure-3body)}$, and the Hamiltonian of the system in the framework of its Center of Mass $H_{rel}^{(pure-3body)}$. Following the method exposed in [12] by applying the change of variable (5), $H_{rel}^{(pure-3body)}$ is transformed into $\widetilde{H}_{rel}^{(pure-3body)}$:

$$
\begin{aligned}
\widetilde{H}_{rel}^{(pure-3body)} =& \frac{2\hbar^2a^2}{m}\left[\sum_{j=1}^{3}\left(z_j\frac{\partial}{\partial_{z_j}}\right)^2\right. \\
&\left. + \mu\sum_{\substack{j,k=1 \\ j\neq k}}^{3}\frac{z_j+z_k}{z_j-z_k}\left(z_j\frac{\partial}{\partial_{z_j}}\right)\right]. \qquad (18)
\end{aligned}
$$

5.1 three identical distinguishable fermions with pure three-body interactions

The eigenfunction of $\widetilde{H}_{rel}^{(pure-3body)}$ for three distinguishable fermions read [12]:

$$
\begin{aligned}
\psi_{rel}^{(pure-3body),fermions}(z_j) =& J_{\{2,1,0\}}^{\mu^{-1}}(z_1,z_2,z_3) \\
&\times \prod_{\substack{j,k=1 \\ j\neq k}}^{3}(z_j-z_k)^{\mu}, \qquad (19)
\end{aligned}
$$

where

$$
\begin{aligned}
&J_{\{2,1,0\}}^{\mu^{-1}}(z_1,z_2,z_3) \\
&\quad = z_1^2z_2 + z_2^2z_1 + z_1^2z_3 + z_3^2z_1 + z_2^2z_3 + z_3^2z_2. \qquad (20)
\end{aligned}
$$

In terms of the variable z_j, Eq. (19) reads

$$
\begin{aligned}
&\psi_{rel}^{(pure-3body),fermions}(z_1,z_2,z_3) \\
&\quad = \left(z_1^2z_2 + z_1^2z_3 + z_2^2z_1 + z_2^2z_3 + z_3^2z_1 + z_3^2z_2\right) \\
&\quad \times [(z_1-z_2)(z_2-z_3)(z_3-z_1)]^{\mu}. \qquad (21)
\end{aligned}
$$

Back to the initial coordinates x_1, x_2 and x_3 by using Eq. (5) and, relative distances $x_{ij} = x_i - x_j$, $i,j = 1,2,3$, Eq. (21) reads:

$$
\begin{aligned}
&\psi_{rel}^{(pure-3body),fermions} = \left(e^{2ia(2x_1-x_2+2x_3)} + e^{6iax_3}\right. \\
&\left. + e^{2ia(2x_2-x_3+2x_1)} + e^{6iax_1} + e^{2ia(2x_3-x_1+2x_2)} + e^{6iax_2}\right) \\
&\times \left[e^{\frac{2}{3}ia(x_1-2x_2+4x_3)} - e^{\frac{2}{3}ia(x_2-2x_3+4x_1)}\right]^{\mu} \\
&\times \left[e^{\frac{2}{3}ia(x_2-2x_3+4x_1)} - e^{\frac{2}{3}ia(x_3-2x_1+4x_2)}\right]^{\mu} \\
&\times \left[e^{\frac{2}{3}ia(x_3-2x_1+4x_2)} - e^{\frac{2}{3}ia(x_1-2x_2+4x_3)}\right]^{\mu}. \qquad (22)
\end{aligned}
$$

After straight forward calculations, the density of probability reads:

$$|\psi_{rel}^{(pure-3body),fermions}|^2 = 2^{(1+3\mu)}\big(3+2\cos 6ax_{23} + 2\cos 6ax_{12}+2\cos 6ax_{31}+2\cos 2a(x_{13}+x_{23}) + 2\cos 2a(x_{31}+x_{21})+2\cos 2a(x_{12}+x_{32}) + \cos 4a(x_{13}+x_{23})+\cos 4a(x_{31}+x_{21}) + \cos 4a(x_{12}+x_{32})\times((1-\cos 2a(x_{13}+x_{23})) \times(1-\cos 2a(x_{31}+x_{21}))(1-\cos 2a(x_{12}+x_{32}))^{\mu} \quad (23)$$

The configurations with null probability corresponding to $|\psi_{rel}^{(pure-3body),fermions}|^2 = 0$ for $a = 0.5$, are shown in Figure 5.

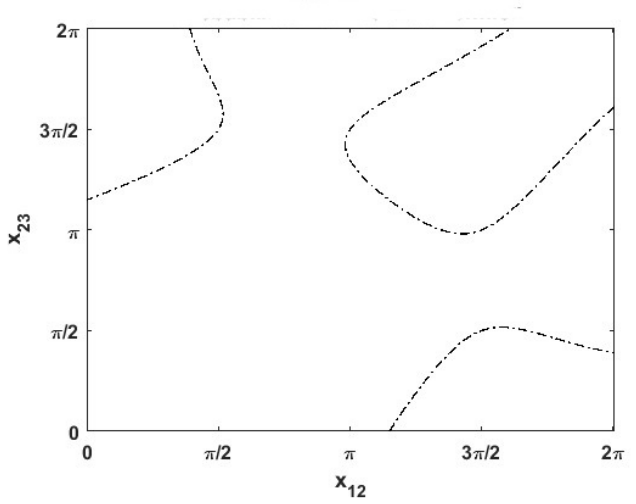

Fig. 5 The configurations with null probability for $a = 0.5$, in the case of three identical distinguishable fermions with pure 3-body interactions. x_{12} is the relative distance between particles labelled 1 and 2 and, x_{23} is the relative distance between particles labelled 2 and 3.

Each of the points of Figure one is a forbidden configuration of the system. For instance the point $x_{12} \approx \frac{3\pi}{2}$, $x_{23} \approx \frac{\pi}{2}$ is a forbidden configuration where angular distances $\widehat{x_1x_2} \approx 270$ and $\widehat{x_2x_3} \approx 90$ degrees.

5.2 three identical distinguishable bosons with pure three-body interactions

In the case of three identical bosons, the eigenfunction of Eq. (18) is

$$\psi_{rel}^{(pure-3body),bosons}(z_j) = J^{\mu^{-1}}_{\{3,0,0\}}(z_1,z_2,z_3) \times \prod_{\substack{j,k=1 \\ j\neq k}}^{3}(z_j-z_k)^{\mu}. \quad (24)$$

Back to the initial coordinates x_1, x_2 and x_3 by using Eq. (5) and, relative distances $x_{ij} = x_i - x_j$, $i,j = 1,2,3$, Eq. (24) becomes

$$\psi_{rel}^{(pure-3body),bosons}(z_j) = \big[2e^{2ia(x_1-2x_2+4x_3)} + 2e^{2ia(x_2-2x_3+4x_1)} + 2e^{2ia(x_3-2x_1+4x_2)}\big]\times \big[e^{\frac{2}{3}ia(x_1-2x_2+4x_3)} - e^{\frac{2}{3}ia(x_2-2x_3+4x_1)}\big]^{\mu}\times \big[e^{\frac{2}{3}ia(x_2-2x_3+4x_1)} - e^{\frac{2}{3}ia(x_3-2x_1+4x_2)}\big]^{\mu}\times \big[e^{\frac{2}{3}ia(x_3-2x_1+4x_2)} - e^{\frac{2}{3}ia(x_1-2x_2+4x_3)}\big]^{\mu}. \quad (25)$$

Straight forward calculations yields:

$$|\psi_{rel}^{(pure-3body),bosons}|^2 = 2^{(2+3\mu)}\big(3 + 2\cos 6a(x_{13}+x_{23})+2\cos 6a(x_{31}+x_{21}) + 2\cos 6a(x_{12}+x_{32})\big)\big((1-\cos 2a(x_{13}+x_{23})) \times(1-\cos 2a(x_{31}+x_{21}))(1-\cos 2a(x_{12}+x_{32}))\big)^{\mu}. \quad (26)$$

The configurations with null probability corresponding to $|\psi_{rel}^{(pure-3body),bosons}|^2 = 0$ for $a = 0.5$, are shown in Figure 6.

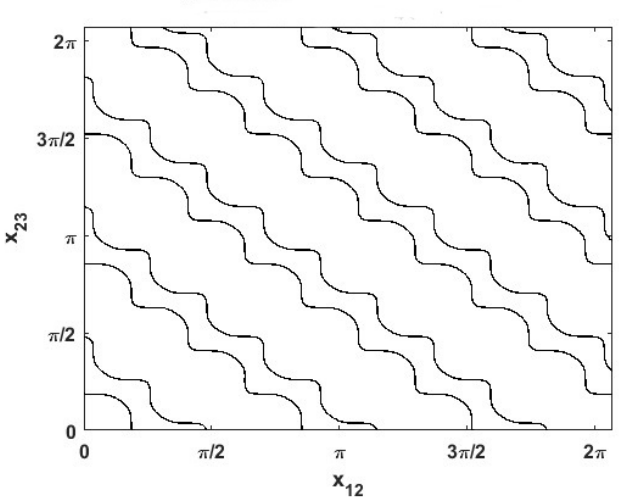

Fig. 6 The configurations with null probability for $a = 0.5$, in the case of three identical distinguishable bosons with pure 3-body interactions. x_{12} is the relative distance between particles labelled 1 and 2 and, x_{23} is the relative distance between particles labelled 2 and 3.

As in previous figures, In Figure 6, any point corresponds to a forbidden configuration. For instance, the point $x_{12} \approx \pi$, $x_{23} \approx \frac{\pi}{4}$ is a forbidden configuration where angular distances $\widehat{x_1x_2} \approx 180$ and $\widehat{x_2x_3} \approx 45$ degrees.

6 Forbidden configurations in the case of pairwise interactions

In the case of pure pairwise interaction, the Hamiltonian of the system (4) is reduced to [23]:

$$H^{pairwise} = \frac{-\hbar^2}{2m}\sum_{i=1}^{3}\left(\frac{\partial}{\partial x_i}\right)^2 + \frac{\hbar^2}{m}\nu(\nu-1)a^2\sum_{\substack{i,j=1\\ i\neq j}}\frac{1}{\sin^2[a(x_i-x_j)]}. \quad (27)$$

Eq. (27) can be written as the sum of $H_{CM}^{pairwise}$ and $H_{rel}^{pairwise}$, Hamiltonian of the centre-of-mass and Relative Hamiltonian, respectively. The relative Hamiltonian can be written as follows [24]:

$$H_{rel}^{pairwise} = -\frac{\hbar^2}{2m}\sum_{j=1}^{3}\left(\frac{\partial^2}{\partial x_j^2}\right) - \frac{\hbar^2}{m}a\nu\sum_{j\neq k}^{3}\cot(ax_{jk})\left(\frac{\partial}{\partial x_j}-\frac{\partial}{\partial x_k}\right) \quad (28)$$

Letting $z_j = \exp(2iax_j)$, Eq. (28) becomes

$$\widetilde{H}_{rel}^{pairwise} = \frac{2\hbar^2a^2}{m}\left[\sum_{j=1}^{3}\left(z_j\frac{\partial_j}{\partial z_j}\right)^2 + \nu\sum_{j\neq k}^{3}\frac{z_j+z_k}{z_j-z_k}\left(z_j\frac{\partial_j}{\partial z_j}-z_j\frac{\partial_k}{\partial z_k}\right)\right]. \quad (29)$$

6.1 three identical distinguishable fermions

For three identical fermions, the eigenfunction of Eq. (28) is

$$\psi_{rel}^{pairwise,fermions}(z_j) = \left(z_1^2z_2+z_1^2z_3+z_2^2z_1+z_2^2z_3+z_3^2z_1+z_3^2z_2\right) \times[(z_1-z_2)(z_2-z_3)(z_3-z_1)]^{\nu}, \quad (30)$$

Back to the initial coordinates x_1, x_2 and x_3 by using Eq. (5) and, relative distances $x_{ij}=x_i-x_j$, $i,j=1,2,3$, the wave function in Eq. (30) reads:

$$\psi_{rel}^{pairwise,fermions} = e^{-2ia(2x_1+x_2)}+e^{-2ia(2x_1+x_3)} + e^{-2ia(2x_2+x_1)}+e^{-2ia(2x_2+x_3)}+e^{-2ia(2x_3+x_1)} + e^{-2ia(2x_3+x_2)}\times\left[(e^{-2iax_1}-e^{-2iax_2})\right. \times\left.(e^{-2iax_2}-e^{-2iax_3})(e^{-2iax_3}-e^{-2iax_1})\right]. \quad (31)$$

Straight forwards calculations yields

$$|\psi_{rel}^{pairwise,fermions}|^2 = 2^{(1+3\nu)}\big(3+2\cos 2ax_{12} + 2\cos 2ax_{23}+2\cos 2ax_{31}+\cos 4ax_{12}+\cos 4ax_{23} + \cos 4ax_{31}+2\cos 2a(x_{31}+x_{21}) + 2\cos 2a(x_{12}+x_{32})+2\cos 2a(x_{23}+x_{13})\big) \times\big((1-\cos 2ax_{12})(1-\cos 2ax_{23})(1-\cos 2ax_{31})\big)^{\nu} \quad (32)$$

The configurations with null probability corresponding to $|\psi_{rel}^{pairwise,fermions}|^2=0$ for $a=0.5$, are shown in Figure 7.

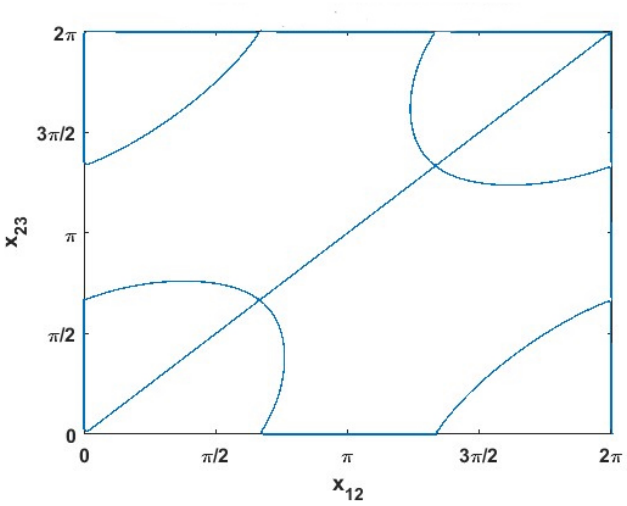

Fig. 7 The configurations with null probability for $a=0.5$, in the case of three identical distinguishable fermions with pairwise interactions. x_{12} is the relative distance between particles labelled 1 and 2 and, x_{23} is the relative distance between particles labelled 2 and 3.

Similar to previous figures, In Figure 7, any point corresponds to a forbidden configuration. For instance, the point $x_{12}=\frac{\pi}{2}$, $x_{23}=\frac{\pi}{2}$ is a forbidden configuration where angular distances $\widehat{x_1x_2}$=$\widehat{x_2x_3}$= 90 degrees.

6.2 three identical distinguishable bosons

For three identical bosons, the eigenfunction of Eq. (28) is

$$\psi_{rel}^{pairwise,bosons} = 2\left[e^{-6iax_1}+e^{-6iax_2} + e^{-6iax_3}\right]\times\left[(e^{-2iax_1}-e^{-2iax_2})\right. \times\left.(e^{-2iax_2}-e^{-2iax_3})(e^{-2iax_3}-e^{-2iax_1})\right] \quad (33)$$

Back to the initial coordinates x_1, x_2 and x_3 by using Eq. (5) and, relative distances $x_{ij}=x_i-x_j$, $i,j=$

1,2,3, Eq. (33) reads:

$$|\psi_{rel}^{pairwise,bosons}|^2 = 2^{(2+3\nu)}\left[3+2\cos 6ax_{12}\right.$$
$$\left.+2\cos 6ax_{23}+2\cos 6ax_{31}\right]$$
$$\times(1-\cos 2ax_{12})(1-\cos 2ax_{23})(1-\cos 2ax_{31}) \qquad (34)$$

The configurations with null probability corresponding to $|\psi_{rel}^{pairwise,bosons}|^2 = 0$ for $a = 0.5$, are shown in Figure 8.

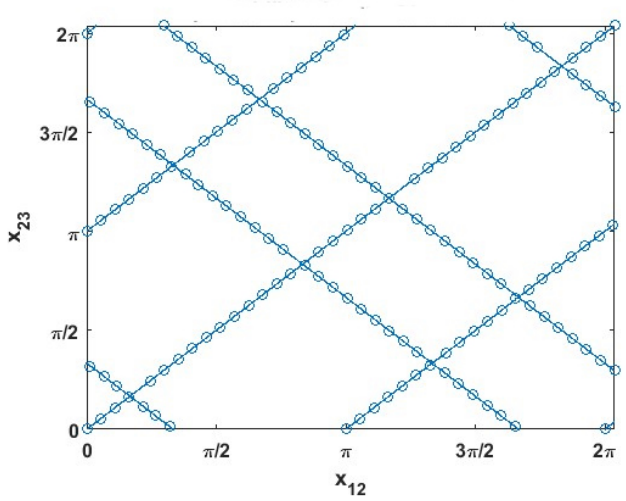

Fig. 8 The configurations with null probability for $a = 0.5$, in the case of three identical distinguishable bosons with pairwise interactions. x_{12} is the relative distance between particles labelled 1 and 2 and, x_{23} is the relative distance between particles labelled 2 and 3.

Figure 7 is a superposition of lines and multitude of small circles on these lines. Any point of these lines or circles constitutes a forbidden configuration of the system. For instance, the equation of one of these lines reads $x_{23} = x_{12}$. Therefore $x_{12} = \frac{\pi}{2}$ constitute a forbidden configuration. i.e. the angular distance $\widehat{x_1x_2}$=$\widehat{x_2x_3}$= 90 degrees is one of the infinite number of forbidden configurations in this case.

7 Conclusions and outlooks

In the three-body quantum problem, an important question is to know which of the pairwise, pure three-body or full three-body interactions best fits a given physical situation. In this paper, we have a strong tool to answer this question by comparing theoretical predictions of forbidden configurations to experimental observations.

To this end, we write explicitly the wave function for three identical distinguishable particles on a ring with the so-called trigonometric interactions. We show that in all cases, there are infinite sets of forbidden configurations associated with the system's null density probability. A configuration corresponds to a given set of relative distances between particles, x_{12} and x_{23}.

These configurations are exhibited in six figures: Figures 3, 5 and 7 represent forbidden configurations for three fermions on a ring in the case of full three-body interactions, pure three-body interactions and pairwise interactions, respectively. Figures 4, 6 and 8 represent forbidden configurations for three bosons on a ring in the case of full three-body interactions, pure three-body interactions and pairwise interactions, respectively.

Given a system with, let's say, three fermions on a ring. The question is, with which kind of interactions, full three-body, pure three-body, or pairwise, should one model the system? Here is the procedure to choose the correct interactions. Experimentally, it is possible to point out some configurations with null probability. These configurations, to experimental uncertainties, will be closed to one of the figures 3, 5 or 7. Hence, this simple comparison will decide which of the three kinds of interactions prevail in this system.

We suggest the context of cold atoms ring-shaped optical lattices as an observational, experimental context [17–19].

References

1. S. Erkoç, Ann. Rev. Comput. Phys. IX **1**, 1 (2001)
2. S. Surulere, M. Shatalov, A. Mkolesia, J. Ehigie, Int. J. Math. Mod. Num. Opt. **10**, (2020)
3. D. Tranh, V. Hoang, T. Hanh, Physica B. **608** (2021)
4. L. Pizzagalli, J. Godet, J. Guénolé, S. Brochard, E. Holmstrom, K. Nordlund, T. A. J. Albaret, J. Phys.. **25**, 1 (2013), https://doi.org/10.1088/0953-8984/25/5/055801
5. J. Holt, M. Kawaguchi, N. Kaiser, Front. Phys. **8** (2020)
6. K. Vacek, A. Okiji, N. Kawakami, *Eigenfunctions for SU(N) particles with 1/r2 interaction in harmonic confinement* (IOP Publishing, 1994)
7. K. Sogo, J. Phys. Soc. Japan. **65** (1996)
8. F. Calogero, C. Marchioro, J. Math. Phy. **15** (1974)
9. M. Rosenbaum, A. Turbiner, A. Capella, Inter. J. Modern Phy. A **13** (1998)
10. C. Quesne, Phys. Rev. A. **55**, 5 (1997)
11. W. Ruhl, A. Turbiner, Mod. Phys. Lett. A. **10** (1995)
12. H. Rahmati, A. Latifi, Few-Body Syst. **60** (2019)
13. M. A. Olshanetsky J. Nonlinear Math. Phys. **12** (2005)

14. A. Polychronakos, *The physics and mathematics of Calogero particles* (IOP Publishing, 2006)
15. G. Gibbons, P. Townsend, Phys. Lett. B **454** (1999)
16. Y. Yu, W. Zheng, Z. Zhu, Phys. Rev. B **56** (1997)
17. L. Amico, A. Osterloh, F. Cataliotti, Phys. Rev. Lett.. **95**, 8 (2005)
18. Y. Yu, Z. Luo, Z. Wang, J Phys Condens Matter **26** (2014)
19. J. Y. Choi, J. Korean Phys. Soc. **82** (2023)
20. B. Sutherland, J. Mathe. Phys.. **12** (1971)
21. B. Sutherland, Phys. Rev. A **4**, 11 (1971)
22. J. Wolfes, J. Math. Phys.. **15** (1974)
23. B. Sutherland, Phys. Rev. A **5**, 3 (1972)
24. L. Lapointe, P. Mathieu, Sym. Integr. Geo. meth. Appl. **11** (2015)
25. F. Lesage, V. Pasquier, D. Serban, Nuc. Phys. B **435** (1995)